SECOND SEMIANNUAL TECHNICAL REPORT

1/1/71 - 6/30/71

STRUCUTRAL EFFECTS ON ELECTRICAL PROPERTIES IN AMORPHOUS SEMICONDUCTORS

School of Engineering
Vanderbilt University
Nashville, Tennessee 37203

D. L. Kinser, Co-principal Investigator 615-322-2413

L. K. Wilson, Co-principal Investigator 615-322-2771

Sponsored by

ADVANCED RESEARCH PROJECTS AGENCY

ARPA ORDER: 1562

PROGRAM CODE: 61101D

CONTRACT NUMBER: DAHC04-70-C-0046

AMOUNT OF CONTRACT: $88,136.00

EFFECTIVE DATE OF CONTRACT: June 1, 1970

CONTRACT EXPIRES: May 31, 1972

Date Submitted: July 31, 1971

ABSTRACT

During this report period, work has been concentrated on a survey of the structure, electrical and magnetic properties of transition metal oxide-phosphate glasses and glasses in the As_2Te_3-As_2Se_3 system which possess electrical or magnetic device potential. Results of magnetic and electrical observations in several transition metal-phosphate glasses have revealed a high degree of magnetic and structural order. The pronounced influence of glass-glass phase separation has also been noted.

Examination of a V_2O_5 - P_2O_5 glass has revealed an anti-ferromagnetic transition in the glass at a low temperature. Results on a CuO-P_2O_5 glass are promising, in that an extremely large range of conductivities has been observed thus indicating potentially useful in device application.

Detailed studies of the As_2Te_3-As_2Se_3 system has shown switching behavior which can be controlled with compositional variation. These results are consistent with a thermally induced switching mechanism. This material has been examined in the microwave frequencies and exhibits an extremely high dielectric constant with low losses.

STATEMENT OF PROBLEM

The device potential in amorphous semiconducting materials is a largely unexploited area, despite extensive research in this area. This is the result of a lack of systematic structure-property oriented research in these materials. A fundamental understanding of the structural features of this class of materials will allow rational interpretation and control of relationships between glass preparation variables and important electrical and magnetic properties.

Electronic conduction in amorphous solids has become the the subject of interest to a number of theoreticians and has been reviewed by Mott (1), Gubanov (2) and numerous others. Virtually all of these works have begun with an assumption that amorphous solids are uniformly random, even though they recognize glasses are generally heterogenous. These theoreticians have developed analytical descriptions of several systems which have been experimentally verified in some cases. Attempts to extend this approach to microscopically heterogenous systems have had notably little success. There remains a considerable body of experimental results, including Hall and Seebeck coefficients, which are not rationalized by present theory.

Pearson (3) has suggested that heterogenous structure in these materials may explain these anomalies if the separated phase is crystalline. It appears that heterogenous transport

analysis similar to that of Volger (4) or Bube (5) is required to ascertain the transport behavior in each phase.

Another important anomaly between theory and observation concerns the theoretically predicted insensitivity of amorphous semiconductors to doping. Early experimental observations by Kolimets, et. al. (6), conformed to the theoretical predictions, but recent work by Mackenzie (7) clearly conflicts with the theory and the early work. It appears that the above anomalies are the result of inadequate structural characterization, rather than fundamental theoretical problems.

Further evidence that structural heterogenities lie at the root of these anomalies can be inferred from work by Kinser, et.al. (8), in K_2O-P_2O_5-V_2O_5 glasses. This work has shown that marked changes in dielectric behavior occur during thermal treatments customarily used to stress relieve glasses. These changes have been shown to be the result of structural changes involving precipitation of small amounts of crystals.

Wilson and Kinser (9) have observed similar, but somewhat more complex, behavior in FeO-P_2O_5 glasses after thermal treatments corresponding to annealing. Electron spin resonance (ESR) results have shown the onset of structural changes during thermal treatment prior to their observation by other commonly employed techniques (10).

It is thus apparent that homogenous glasses, semiconducting

or otherwise, are the exception rather than the rule.

GENERAL METHODOLOGY

The electrical and magnetic property changes accompanying structural modifications during glass processing are of prime interest in the present work. The above questions can only be answered with detailed structural characterization of representative glasses from the oxide and chalcogenide groups. The initial oxide glass examined was the 55 FeO-45 P_2O_5 glass along with glasses from the V_2O_5-P_2O_5, CuO-P_2O_5, TiO_2-P_2O_5 and MnO-P_2O_5 systems. The initial chalcogenide glasses are from the As_2Te_3-As_2Se_3 system wilh Ag-As-s glasses in preliminary stages of study.

Structural characterization of these systems is being accomplished using electron microscopy, Guinier-DeWolff x-ray, electron spin resonance spectroscopy, magnetic susceptibility, electron microprobe, dielectric relaxation, Mössbauer spectroscopy and differential thermal analysis techniques.

In conjunction with the structural tools, it is necessary hat the conductivity, switching behavior and Seebeck coefficient be monitored to allow direct structure-property correlations.

RESULTS

Transition Metal Phosphate Glasses

Previously reported work in $FeO-P_2O_5$ glasses has indicated that considerable compositional segregation occurs during thermal treatments. Simliar compositional segregation has also been previously inferred in $V_2O_5-P_2O_5$ glasses.

$FeO-P_2O_5$ Glasses

Electrical resistivity has been observed in a $55FeO-45P_2O_5$ glass for a series of oxidation states with differing thermal treatment temperatures (See paper appended for detailed discussion). The results of these observations have indicated that the minima in the conductivity versus oxidation state plot (Figure 1) is shifted after themal treatment. Chemical analysis of samples before and after thermal treatment show no change in overall oxidation state. These observations indicate that this system segregates preferentially in a manner which appears to shift the minimum in resisitivty to about $Fe^{3+}/Fe^{total}=0.7$. This shift is clearly a consequence of microstructural segregation and not a consequence of the atomic structure of the glass.

Magnetic susceptibility of the iron-phosphate glasses revealed that the iron ions in the bulk glass were coupled antiferromagnetically with $\theta = -239^{o}K$ and $\chi = 6.58 \times 10^{-5}$ cgs. At room temperature these results are in accord with previous ESR data which indicated that the iron ions in the bulk glass were

coupled antiferromagnetically in trivalent and divalent pairs. Heat treatment of the glasses for 14 hours at 800°C resulted in devitrification and growth of crystalline phases which have been identified by room temperature vacuum Guinier de Wolff techniques as Fe_3O_4, $FePO_4$, Fe_3PO_7, and $Fe_4(P_2O_7)_3$. The heat treatment caused the projected θ to decrease to -74°K and the mass susceptibility to increase to 7.18×10^{-5} cgs.

V_2O_5-P_2O_5 Glasses

Glass formation in the V_2O_5-P_2O_5 system was initially reported by Roscoe (11) in 1868. Almost a century later Munakata (12) examined a 60 V_2O_5 -20 P_2O_5 -20 BaO glass with varying V^{4+}/V^{5+} ratio and observed a minimum in resistivity at V^{4+}/V^{total} = 0.2 Several others have subsequently discussed the significance of this observation in terms of the conduction mechanism (13,14). Recently Lindlsey et.al. (15) have published a comprehensive analysis of five different V_2O_5/P_2O_5 compositions with varying V^{4+}/V^{total} ratios. Lindsley observed a minimum in resistivity in all glasses examined in the range $V^4/V^{total} \simeq 0.1$-0.2.

It appears that the observation of this deviation of the minimum point from 0.5 is quite damaging to a single hopping conduction model; Lindsley proposed two possible explanations to salvage the hopping model. The first consists of a complex ion formation which structurally isolates some of the V^{5+} from the conduction process. The second possible explanation depends

upon the structural breakup of -V-O-P-chains. Neither of these explanations is particularly palatable in the light of the strong glass forming tendency of both V_2O_5 and P_2O_5.

Lindsley et.al. cited a recent work by Anderson & Luehrs(16) as indicating microscopic homogenity. This work was conducted on thin films which in fact exhibited some phase separation characteristics. We have examined numerous V_2O_5/P_2O_5 glasses using electron replica techniques on fractured etched surfaces and almost all of the glasses examined exhibit immiscibility.

An extensive magnetic study of the vanadium-phosphate glass system was undertaken in an attempt to resolve some discrepancies in the literature. Several investigators (17,18) have reported hyperfine spectra in their ESR data of 90-10 and 80-20 vanadium-phosphate glasses. Glasses with these compositions were made, but no hyperfine structure was observed. Eventually 6 glasses were studied in the 60-90 mole % V_2O_5 range and the microstructures revealed the presence of a mestable immiscibility gap. In spite of the extensive phase separation in the glasses containing high vanadium concentrations, no hyperfine structure was observed. Since none of the investigators who detected hyperfine reported any x-ray studies of their glasses, we have concluded that their samples were partially devitrified.

It was determined by correlation of magnetic susceptibility and ESR data that there existed direct antiferromagnetic coupling

between V^{4+} ions in the glass. This coupling resulted in an antiferromagnetic transition temperature near - 70°C. The reduction in temperature of this transition temperature from the Neel temperature of crystalline VO_2 is the result of the octahedral site symmetry of the V^{4+} in the glass and the delocalization of the V-O bonding electrons by the phosphorous ion.

Determination of the concentration of V^{4+} ions in the glasses studied was in agreement with two previous investigators (19,20). However, it was found that the linewidth of the resonance increased at high vanadium concentrations. This is contrary to the prediction of the generally accepted structural model proposed by Janakirama-Rao (21). The linewidth increase is the result of inhomogeneity broadening due to the increased phase separation of glasses containing high vanadium concentrations. Thermal treatments leading to phase separation of the glasses also caused a hysteresis in the resonance intensity vs. temperature plot at the antiferromagnetic transition temperature. This hysteresis is similar to that observed in the Neel temperature of crystalline compounds containing more than one phase (22).

In order to study the magnetic behavior of glasses with increased concentration of the lower valence state ions, dextrose was added to the melts of the 65-35 and 80-20 glasses. This resulted in enhanced phase separation of the glass into vanadium-rich and phosphate-rich phases. A hysteresis was observed at the

transition temperature of the glass, and in addition, weak transitions were observed at +70° and -120°C, the Neel temperatures of VO_2 and V_2O_3, respectively. These weak transitions indicate that the addition of dextrose to the melt produced V^{4+} and V^{5+} ions and also that the local lingand environments of these trivalent and tetravalent ions in the separated phase were quite similar to the local ligand environments in V_2O_3 and VO_2. Thus V^{4+}-V^{4+} and V^{3+}-V^{3+} antiferromagnetic coupling in the separated phase resulted in transitions similar to those observed in crystalline systems. A paper discussing the magnetic behavior of these glasses is appended.

$CuO-P_2O_5$ Glasses

A 55 $CuO-55P_2O_5$ glass has been prepared with varying Cu^{2+}/Cu^{total} ratio. The electrical conduction process in these glasses is not presently clear as both large activation energies for conduction (0.80-1.0ev) and minor time dependent conduction have been observed. The electrical conductivity of these glasses will continue to be studied since it appears that the conduction mechanism may be both electronic and ionic in these glasses. It was also observed that the resistivity appears to minimize near $Cu^{2+}/Cu^{total} = 0.4$. This behavior appears similar to the other transition metal oxide-phosphate glasses.

Investigations of a 55-45 mole % MnO_2-P_2O_5 glass have led to a preliminary characterization of the magnetic structure of the material. The glass was prepared in a manner similar to that employed with other glasses studied; however, it was found that the conductivity was less than 7×10^{-15} $(ohm\text{-}cm)^{-1}$ This implied that practically all of the maganese is in one valence state, in sharp contrast to the iron and vanadium-phosphate glasses, where as much as 50% of the transition metal ion was in the lower valence state in the as cast glass.

Magnetic susceptibility measurements of the manganese-phosphate glass showed that the bulk properties are antiferromagnetic with a projected $\theta = -230^{\circ}K$, $\chi = 8.05 \times 10^{-15}$ (cgs units) at room temperature, and $C = 3.71 \times 10^{-2}$. However, the ESR line intensity vs. temperature plot indicated that the glass is ferromagnetic down to $21^{\circ}K$. In addition, a calculation of the area under the absorption spectra to determine the spin density yielded a valve which is 10^3 greater than the number of spins in the sample.

We have concluded that the manganese ions in this manganese-phosphate glass are strongly antiferromagnetically coupled in pairs. Yet because of local site distortion there is a slight noncolinearization of the spins. The resultant moment from each pair couples with other resultant moments so that a ferromagnetism is thought to exist with a transition temperature less

than 21°K. The discrepancy between the spin density calculated from stochiometry and from ESR data is the result of the strong internal molecular field in the glass.

$TiO-P_2O_5$ Glasses

Glass formation in this system was reported in the literature only recently, and little property work has been published to date. The main difficulty in this system arises in preparation of specimens, due to the difficulty of obtaining a homogeneous amorphous structure. J. R. Pawlik, et.al. (23) recently presented A.C. and D.C. conductivity for a 4.5 TiO_{2-x} $2.0P_2O_5$ glass of varying x-value as a function of a temperature and frequency. If their D.C. data is replotted as a function of Ti^{3+}/Ti^{total}, it appears that a minima occurs in the range $Ti^{3+}/Ti^{total} > 0.50$. This glass thus appears to behave similarly to the CuO/P_2O_5 glasses.

We have made attempts to study the magnetic properties of titanium-phosphate glasses containing differing relative concentrations of divalent and trivalent ions. The glasses were prepared by prereacting TiO_2 and H_3PO_4, drying the product and melting. In order to obtain Ti^{3+} in the glass, Ti_2O_3 was added to the product of the prereaction. The magnetic susceptibility of all glasses indicated that they were diamagnetic, and ESR studies showed that only a minute quantity of the titanium in the glass was in the trivalent, or paramagnetic state. Thus,

our study of titanium-phosphate glass containing varying concentrations of the valence states of titanium is presently incomplete. However, an ESR study of the glasses will result in valuable information. Since there is such a small quantity of the paramagnetic ion in the glass, exchange coupling between titanium ions would be negligible and we can examine the site symmetry of the isolated Ti^{3+} in the titanium-phosphate glass.

Summary of Transition Metal Phosphate Glasses

From the electrical and microstructural features of the systems thus far examined it appears that if the effects of microstructure are accounted for, the simple hopping model for conduction is applicable. The previous observations of resistivity minima at other than equal ion concentrations appear to be a consequence of micro segregation. The magnetic property observations likewise indicate that considerable confusion has resulted from previously incomplete microstructural and x-ray characterization.

As_2Te_3 - As_2Se_3 Glasses

Previously reported work in the $80As_2Te_3$ - $20As_2Se_3$ has shown memory switching behavior in bulk glass samples. This breakdown voltage was observed to be independent of thickness. During the present report period considerable electrical and structural characterization of glasses in this system has been accomplished.

Delay Time Measurements

Switching delay time measurements were performed on the 80:20 glass and the 70:30 glass by applying a voltage pulse across the sample through a series 100K resistor. The applied voltage and the voltage across the sample were simultaneously observed on a dual-beam oscilloscope. Figure 2 shows the results of a measurement on the 70:30 glass. Two interesting results are apparent from this measurement. First, the threshold switching voltage for the pulsed case is nearly a factor of two higher than it is for the DC or steady state switching (24). Second, it is found that for values of applied voltage slightly greater than the threshold value, the switching delay time is extremely slow, ranging from 600 ms for the 70:30 sample to several seconds for some of the 80:20 glasses. This long switching delay time further supports the idea of a thermally initiated switching process. The type of switching shown in Figure 2 agrees well with the switching predicted by Warren (25) on the basis of his solution of the time-dependent heat-flow equation.

The delay time was found to decrease sharply with increasing

applied voltage, reaching the low millisecond region with over voltages of several hundred volts. The delay time was also found to decrease when a given sample was subjected to repeated breakdown at the same applied voltage. This appears to result from areas of remnant crystallization brought about by the relatively high currents associated with the pulsed switching. Similar behavior with respect to breakdown voltage had been observed earlier in the steady-state switching of the 80:20 and 70:30 glasses (26) and is not surprising in view of the relatively unstable nature of these tellurium-rich glasses. The 60:40 and 50:50 glasses will probably exhibit considerably more stability under pulsed switching, but unfortunately it would require inordinately high values of applied voltage to make the measurements on these samples.

Figure 3 shows the results of the delay-time vs. applied voltage measurements on the 80:20 glass. Curve 1 is for the virgin sample, which exhibits a very long initial switching delay time which then decreases sharply with increasing voltage. Above around 550v, the rate of decrease levels off. Curves 2 and 3 are subsequent runs taken on the same sample. It is seen that the behavior for low voltages is quite different for the three curves, but that at higher voltages all the curves converge. The general behavior of these samples with respect to switching agrees with results reported in the literature for other glasses (27).

Breakdown Voltage Vs. Composition

Breakdown voltage was measured as a function of composition

over the compositional range from pure As_2Te_3 to $40As_2Te_3:60As_2Se_3$. Thermal breakdown theory predicts a breakdown voltage which is independent of thickness for bulk samples. This prediction was confirmed by the measurements, in which the breakdown voltage was found to be essentially independent of the thickness. In addition, breakdown voltage was found to increase markedly with reduction of tellurium content. Figure 4 shows the results of these measurements. Although there is some scatter in the breakdown voltages of different samples with the same composition, the compositional trend is obvious. It was also found that increasing Se content made the glass a much more stable switch at the expense of much higher breakdown voltages. The 50-50 glass, for example, exhibited a very stable breakdown voltage over many breakdown cycles so long as the sample was not subjected to extremely high on-state currents. Since the instability of the 80:20 and 70:30 glasses is believed to be due to localized regions of current-induced crystallization, it is not surprising that the 50-50 glass behaves more uniformly in view of its higher stability as a glass.

Switching Behavior Vs. Temperatures

The switching characteristics of the entire glass system have been studied as a function of temperature. Figure 5 shows the results of increasing temperature on the I-V characteristics of a 50:50 sample. Picture A, taken at room temperature, indicates a very high off-state resistance (> 10MΩ) and no breakdown with an applied voltage in excess of 1000v. Pictures B, C and D, taken at 65°C, 102°C and 123°C, respectively, show successive decreases in the off-state resistance and breakdown voltage as

the temperature rises. In picture E, taken at 140°C, the off-state and on-state resistance are approaching one another in magnitude and the breakdown voltage has fallen to below 100v. Finally, as the temperature is increased further, the sample crystallizes and switching ceases. The resistance of the crystalline state, shown in Picture F, is extremely low. After crystallization, the sample remains in the low resistance state as the temperature decreases.

Figure 6 shows a plot of breakdown voltage vs. temperature for the 60:40 glass. If the heat flow equation is solved for the breakdown voltage, an exponential integral results which can be simplified for temperatures below the glass melting point to give the following expression:

$$V_{BR} = \pi \left(\frac{k\kappa}{\sigma_o \Delta E}\right)^{\frac{1}{2}} \tau \exp(\Delta E/2k\tau) \qquad (1)$$

where k = Boltzmann's constant, τ is the ambient temperature, κ is the thermal conductivity of the glass, σ_o is the infinite temperature electrical conductivity, and ΔE is the activation energy. This equation has been developed and reported in the literature by several researchers (28,29). Equation 1 neglects the field-dependent term, which is essentially equal to unity for a bulk sample. Efforts to fit data such as that shown in Figure 6 to the results predicted by Eq. 1 have been very successful, yielding a very good fit and also producing values of ΔE and $\frac{k}{\sigma_o}$, which were taken as the variable parameters of the fitting process.

D.C. Conductivity

The D.C. (off-state) conductivity of the glass system for $40As_2Te_3:60As_2Se_3$ to $80As_2Te_3:20As_2Se_3$ has been measured over the the temperature range 23°C to 100°C. Preliminary analysis of the data indicates that the D.C. conductivity, σ, of each glass varies exponentially with temperature according to the relation

$$\sigma = \sigma_o \exp \frac{-\Delta_E}{k\tau} \qquad (2)$$

Apparent values of activation energy calculated from $\ell n\sigma$ versus $1/\tau$ curves agree closely with values determined from the switching experiment. The activation energy for each glass was found to generally decrease with increasing tellurium content as might be expected. Table 1 summarizes the electrical data obtained from computer analysis of the experimental data. These measurements will be continued in the low temperature range in order to obtain more accurate values for σ_o and ΔE.

Electron Microscopy

All of the As_2Te_3-As_2Te_3 glasses discussed above have been examined using etched replica electron microscopy techniques. While this work has not been analyzed in detail, it is presently clear that composition changes effect the phase separated microstructures observed. This work will be completed early in the next report period and will be included in the next report.

RECOMMENDATIONS

1. Our principal recommendation is to continue the present program in its present direction to allow the synthesis of each of the results in a unified theory along the lines which are now clear in the chalcogenide system.

2. As in our previous recommendations, we continue to recommend the survey preparation of new glasses. We anticipate that the transition metal oxide-phosphate, silicate, borate and germanate survey presently in progress will be continued.

It is also anticipated that results on a new system Ag-As-S will be most helpful in developing switching models. A detailed ternary phase diagram was recently published (30) and our analyses should be simplified with this as a basis. It is further anticipated that Cu and Au substituted in the above system will be quite informative from an atomistic and microstructural model point of view.

3. The Mössbauer technique should be used to examine 57 Fe and 127 Te in each of the systems presently under examination using other techniques. This will significantly aid in atomic structure model development in these systems as an addition to the present tools.

4. We recommend that the microwave and far infrared "conductivity spectra" be obtained to facilitate in theoretical analysis of the conductivity/loss spectra. This will allow the loss behavior to be explicitly attributed (31) to each mechanism thus reinforcing both atomic and microstructural analyses.

REFERENCES

1. N. F. Mott, "Conduction in Non-Crystalline Systems I & II," Phil. Mag. 117, 1259-1284 (1968).

2. A. Gubanov, "Quantum Theory of Amorphous Semiconductors," Translated by A. Tubylewicz, Consultants Bureau, New York (1965).

3. A. D. Pearson, "The Hall Effect - Seebeck Effect Size Anomaly in Semiconducting Glasses," J. Electrochem. Soc. 111 (6) pp.753-755, (1964).

4. J. Volger, "Note on Hall Potential Across an Inhomogenous Conductor," Phys. Rev. 79, pp.1023-1024 (1950).

5. R. Bube, "Interpretation of Hall and Photo-Hall Effects in Inhomogenous Materials," Appl. Phys. Lett. 13 (4) pp.136-139 (1960).

6. B. N. Kolimets, X. Manontova and T. F. Nazarova, "The Structure of Glass," 11, Consultants Bureau, New York (1960).

7. J. D. Mackenzie, "Electronic Conduction in Non-Crystalline Solids," J. Non-Crystalline Solids 2 pp.16-26 (1970).

8. D. L. Kinser, L. L. Hench and A. E. Clark, "Effect of Heterogenities on the Electrical Behavior of a Semiconducting Glass," to be submitted to Journal of Electrochemical Society.

9. L. K. Wilson and D. L. Kinser, "Structure Dependence of Electrical and Magnetic Properties of Iron-Phosphate Semiconductor Glasses," Proc. Region III IEEE Conference, November, 1969.

10. E. J. Friebele, L. K. Wilson, A. W. Dozier and D. L. Kinser, "Antiferromagnetism in an Oxide Semiconducting Glass," Phys. Stat. Sol. (B) 45, 323- (1971).

11. H. E. Roscoe, "Researches on Vanadium," Phil. Trans. Roy. Soc. 158 (1) 1-27 (1868).

12. Munakata, M., Solid State Electronics 1 159 (1960).

13. Baynton, et al. J. Elect. Chem. Soc. 101 237- (1957).

14. Joffee, A. F. Soc. Phys. Sol. St. 2 609 (1960).

15. G. S. Lindsley, A. E. Owen and F. M. Hayatee, "Electronic Conduction in Vanadium Phosphate Glasses," J. Non-Crystalline Solids 4 208-219 (1970).

References Continued

16. G. W. Anderson and F. V. Luehrs, J. Appl. Phys. 39 1634- (1968).

17. V. M. Nagier, Soc. Phys. Sol. State 7, 2204-2206 (1966).

18. Flynch, M. Sayer, S. L. Segel, G. Rosenblatt, to be published J. Appl. Phys. 42 (1971).

19. J. D. MacKenzie, "Semiconducting Glasses," Tech. Rpt. 5, Contract Nonr 591(21).

20. F. R. Landsberger and P. J. Bray, J. Chem. Phys. 53, 2757-2768 (1970).

21. Bh V. Janakirama-RaO, J. Am. Ceram. Soc. 49 605-609 (1966).

22. L. R. Maxwell and T. R. McGuire, Rev. Mod. Phys. 40 714-736 (1953).

23. J. R. Pawlik and T. Y. Tien, "Electrical Behavior of TiO_2-P_2O_5 Glasses," Fall Glass Division Meeting - American Ceramic Society, 1970.

24. H. L. Sanders, L. K. Wilson and D. L. Kinser, "Lm Field Switching and Memory Phenomena in an Amorphous Semiconductor," Proceedings of the 9th Annual Region III IEEE Convention, pp.429-433 (1971).

25. A. C. Warren, "Thermal Switching in Semiconductor Glasses," J. Non-Crystalline Solids 4, 613-616 (1970).

26. Sanders, Wilson and Kinser, op.cit.

27. M. Sugi, M. Kikuchi and S. Sizima, "Switching Characteristics of Chaleogenide Glass," Solid-State Communication 7, 1805-1807 (1969).

28. K. W. Bäer and S. R. Onshinsky, "Electrothermal Initiation of an Electronic Switching Mechanism in Semiconducting Glasses," J. Appl. Phys. 41 (6), 2675-2681 (1970).

29. W. W. Sheng and C. R. Westgate, "On the Preswitching Phenomena in Semiconducting Glasses," Sol. State Comm. 9, 387-391 (1971).

30. G. W. Roland, "The System Ag-As-S: Phase Relations Between 920° and 575°C," Met. Trans. 1 July 1970, p.1811.
G. W. Roland, "Phase Relations Below 575°C in the System Ag-As-S," Economic Geology 65 (3) May 1970, 241.

31. D. L. Kinser, "Electrical Conduction in Glass and Glass Ceramics," in Physics of Electronic Ceramics, Marcel Dekkar, New York, 1971.

TABLE I

Summary of Electronic Data on Chalcogenide Glasses

in the System x As_2Te_3 (1-x) As_2Se_3

Composition	ΔE(ev)	K/σ_o	σ_o $(\Omega^{-1}m^{-1})$
80:20	0.47	1.85×10^{-6}	7.4×10^{4}
70:30	0.40	3.02×10^{-5}	5.48×10^{5}
60:40	0.45	3.00×10^{-5}	2.75×10^{4}
50:50	0.52	7.56×10^{-6}	3.20×10^{1}
40:60	(0.55)*	--	1.98×10^{2}

* From conductivity data

TABLE II

Summary of DTA Observations of Chaleogenide Glasses

	Observed Exothermic Reaction Temperature (^{o}C)		
As_2Te_3/As_2Se_3	5 C^{o}/min	10 C^{o}/min	25 C^{o}/min
80/20	149	172	180
70/30	196	220	225
60/40	213	241	239(?)
50/50	205	N.O.	250(?)
40/60	N.O.	N.O.	N.O.

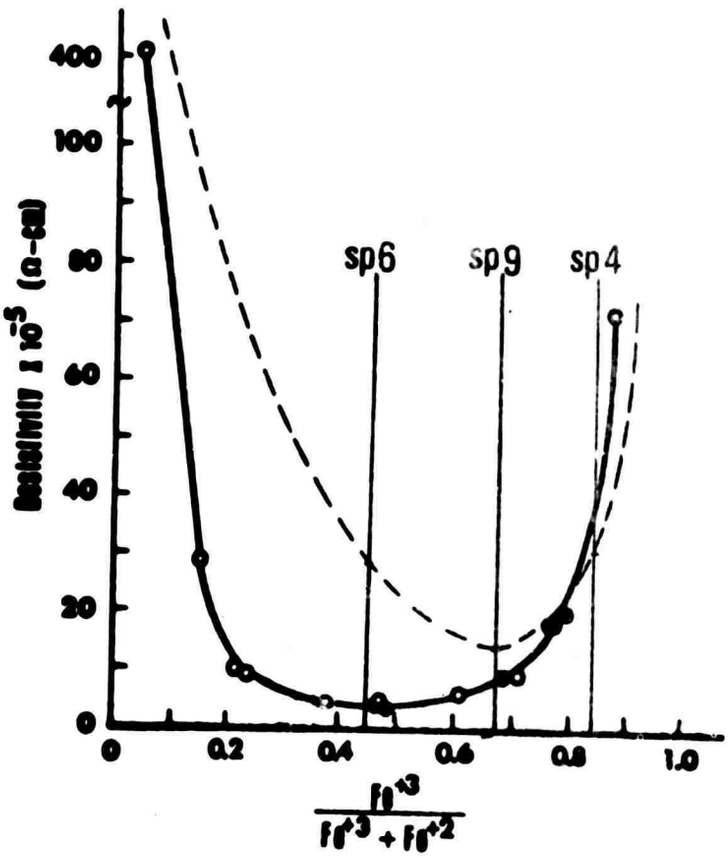

Figure 1. D.C. resistivity at 200°C vs. Fe^{3+}/Fe^{Total}. The data of Hansen is shown with present data after thermal treatment of 1 hour at 600°C.

Figure 2. Delay time measurement of $70As_2Te_3:30As_2Te_3$ glass at room temperature. (Upper trace is applied pulse. Lower trace is voltage across the sample. Time scale:200 ms/cm)

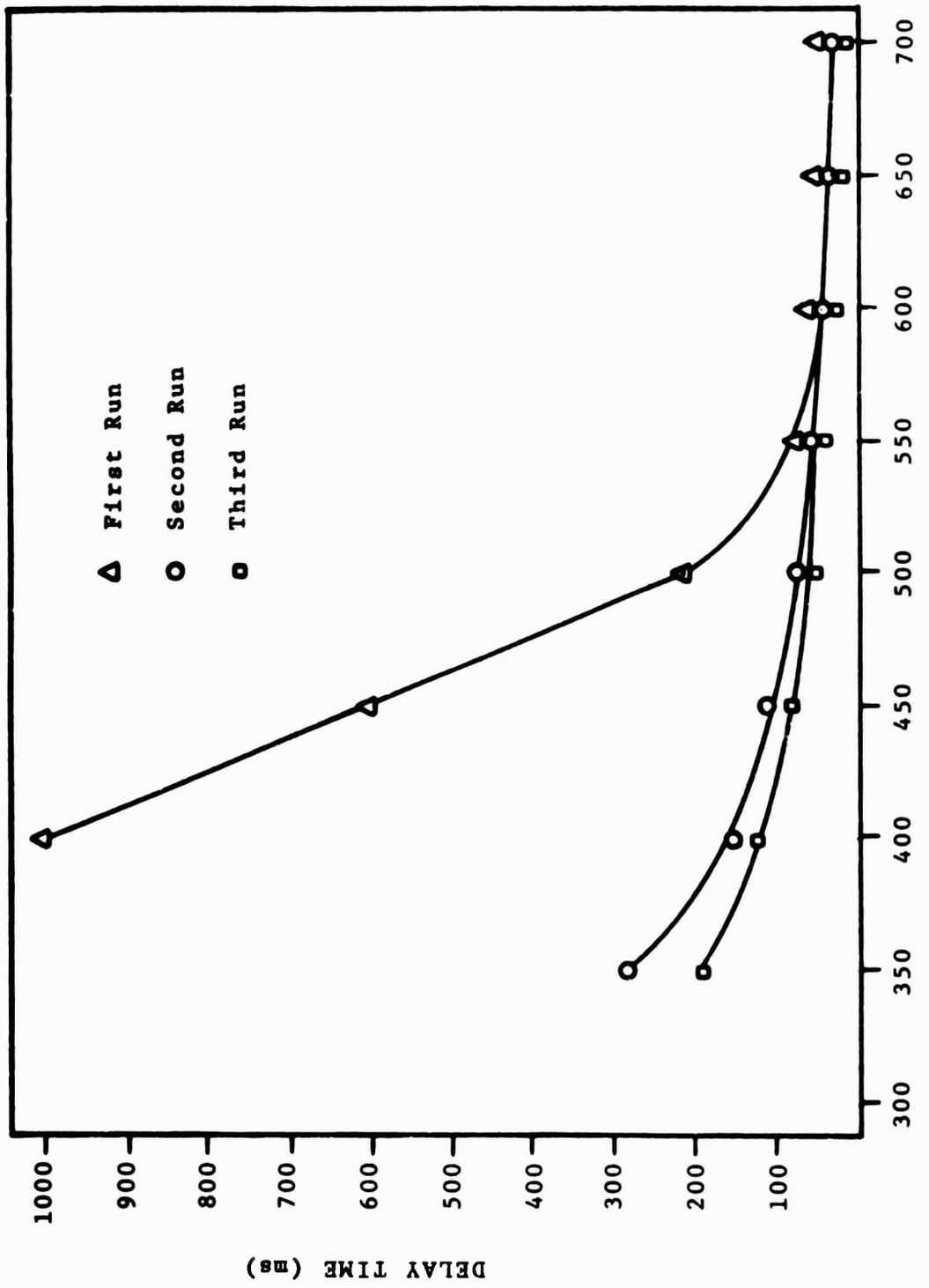

Figure 3. Switching delay time vs. applied voltage for $80As_2Te_3:20As_2Se_3$ glass.

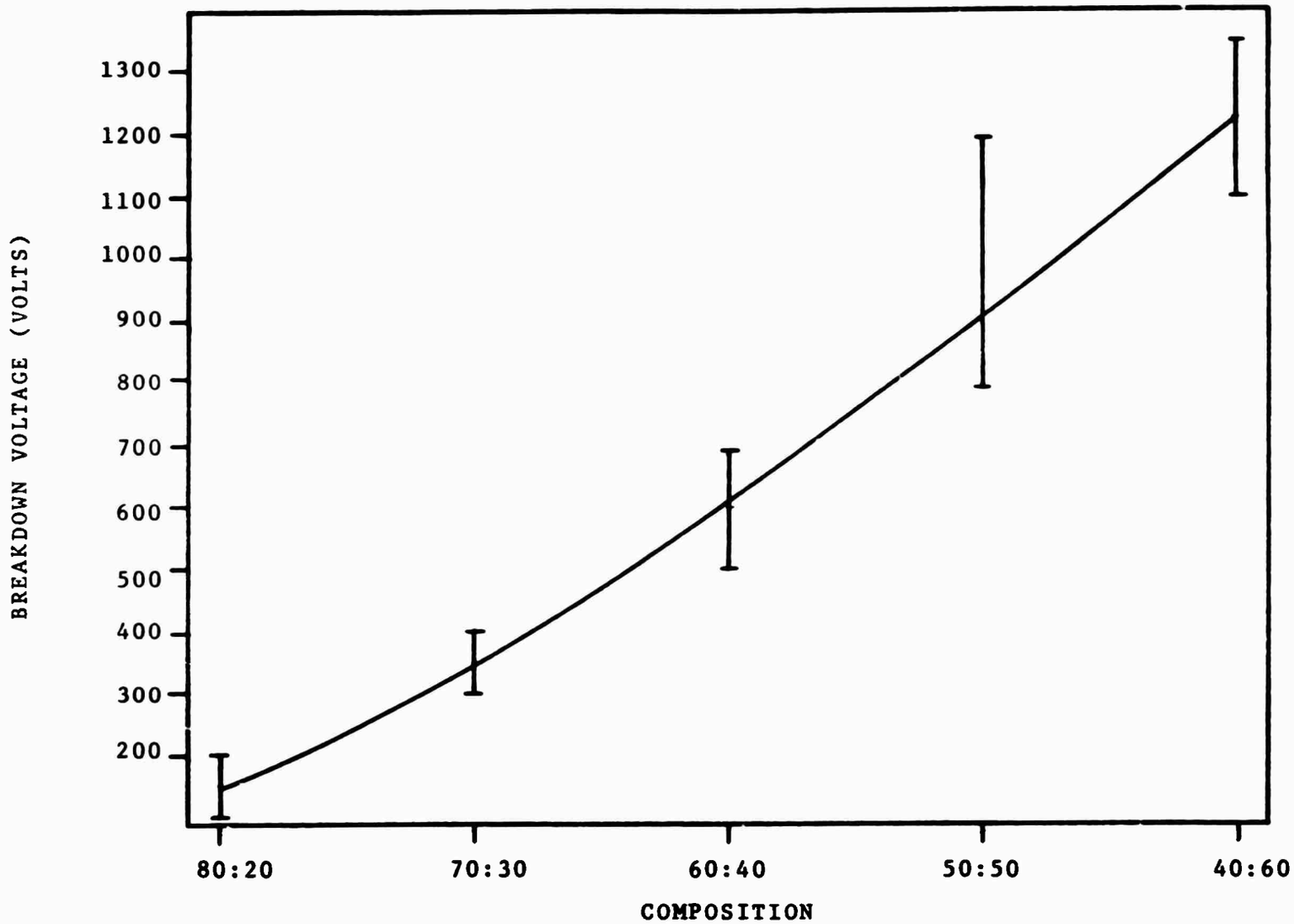

Figure 4. Breakdown voltage vs. composition for the As_2Te_3:As_2Se_3 system. (Error bars indicate results of measurement of several samples.[2] Single sample observations show little scatter.

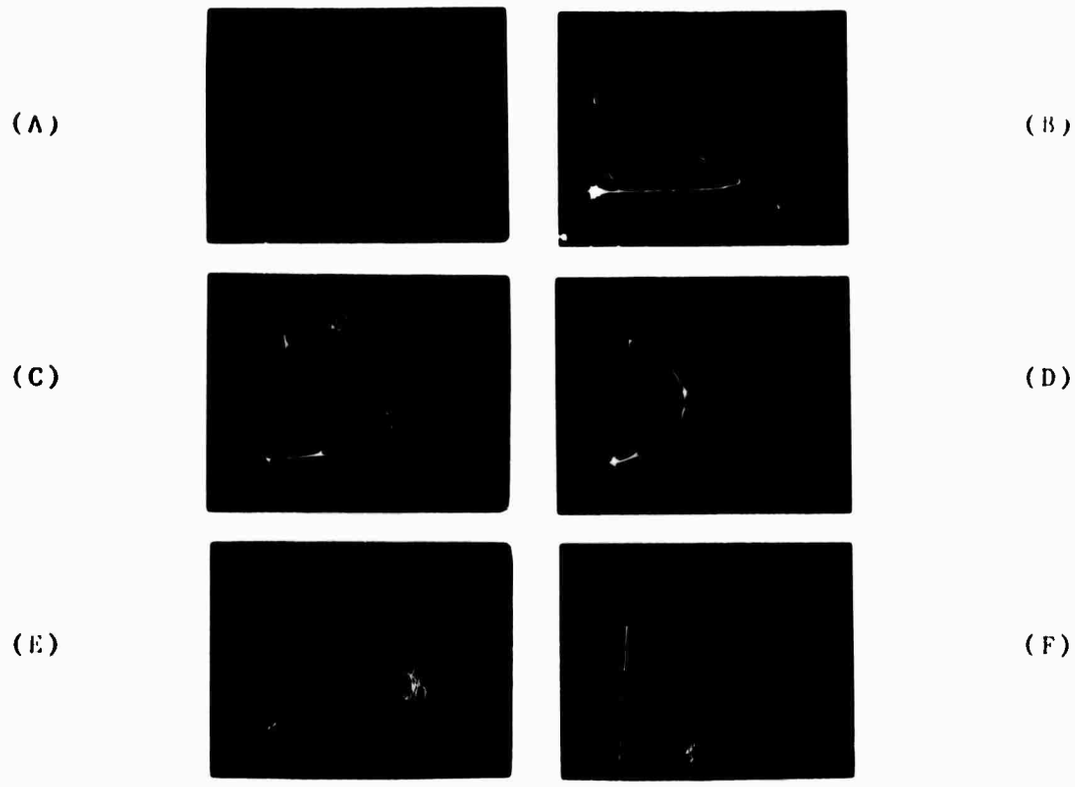

Figure 5. Switching characteristics of $50As_2Te_3$: $50As_2Se_3$ glass at several temperatures (A) 23°C (B) 65°C (C) 102°C (D) 123°C (E) 140°C (F) 165°C

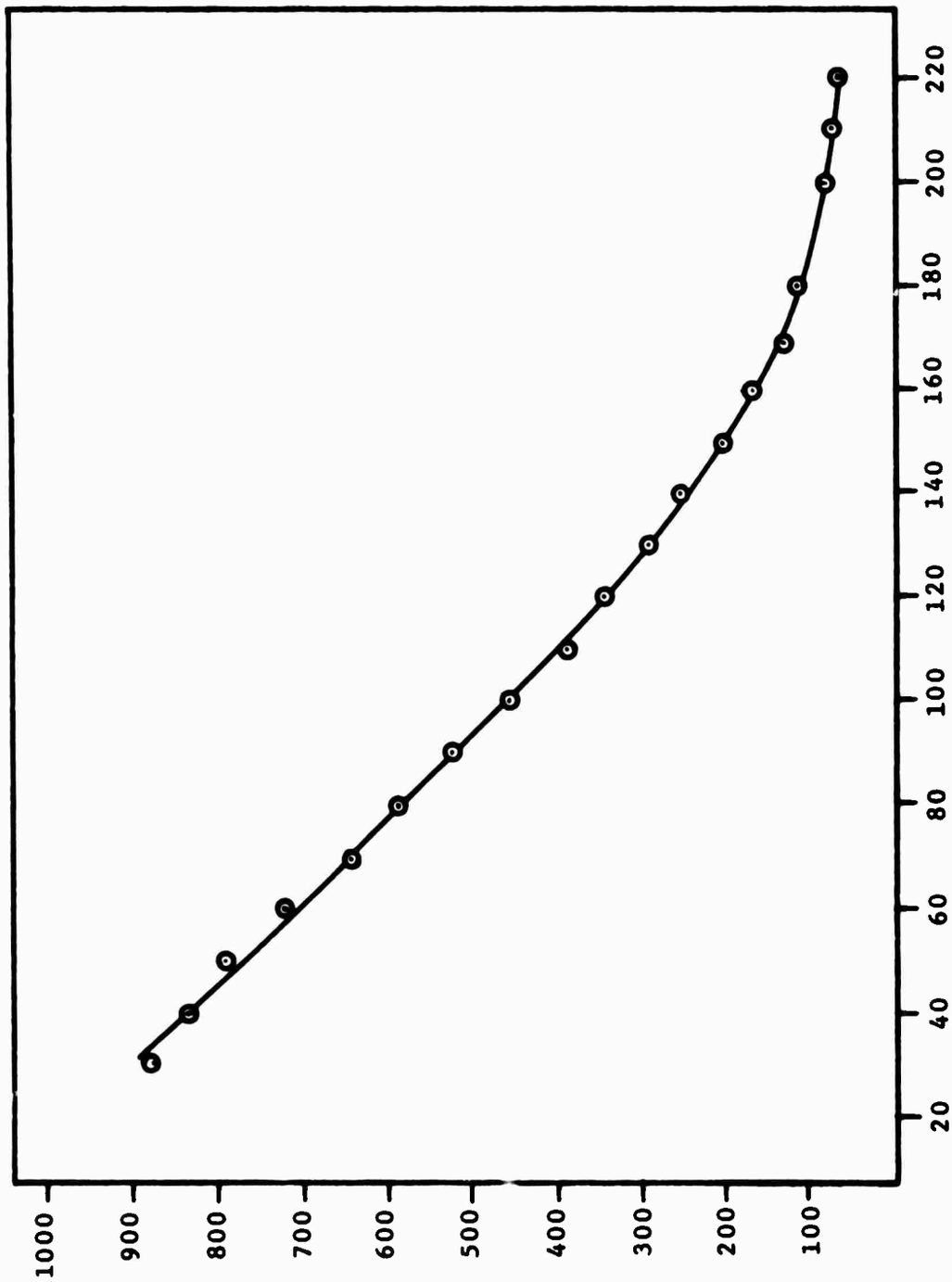

Figure 6. Breakdown voltage vs. temperature for 50-50 glass.

ABSTRACT

Periodic Behavior of Electrical Properties in Transition Metal Phosphate Glasses

A. W. Dozier and D. L. Kinser

The ac and dc electrical properties of representative altervalent transition metal oxide phosphate glasses were surveyed. Glasses of nearly all one ion species, i.e. Mn^{2+}, exhibit extremely high resistivities similar to previous observations in $FeO-P_2O_5$ glasses. Minima in resistivity vs oxidation state plots appear to be correlated with the number of valences available in each system. Low resistivities were observed in surface films on CuO glasses where oxidation/reduction reactions occurred during low temperature treatments. The ac properties of some of these systems exhibit relaxation maxima in the frequency 10^2 to 10^6 Hz, while others are loss free in this range. Electron microscopy of these glasses indicates that microstructural features can explain all observed relaxation maxima.

This paper was presented to the Glass Division, American Ceramic Society Meeting, April 26, 1971 in Chicago, Illinois.

ANTIFERROMAGNETIC BEHAVIOR IN THE V_2O_5-P_2O_5 SEMICONDUCTING GLASS SYSTEM

E. J. Friebele, L. K. Wilson and D. L. Kinser

Vanderbilt University
Nashville, Tennessee 37203

The magnetic resonance spectra of the semiconducting glass system $x\ V_2O_5 \cdot (1-x)\ P_2O_5$ ($x = 0.80$, 0.75, 0.70, 0.65, and 0.60) has been studied as a function of experiment temperature at 9.0 GHz. The resonance spectra of the glasses consist of a singlet with approximately 300 gauss linewidth centered near $g' = 1.96$. The linewidth and the g' values for each glass were essentially constant over the temperature range 77° K to 400° K. Both annealed and unannealed glasses exhibited antiferromagnetic behavior with anomalies in the spectra line intensities at temperatures corresponding to known antiferromagnetic transitions in the pure phase vanadium oxides. The magnetic resonance data has been explained in terms of a proposed structural model for the V_2O_5-P_2O_5 glass system. (Research sponsered by the U.S. Army Research Office-Durham)

Abstract submitted to the Annual Meeting of the American Ceramic Society, March, 1971.

Paper to be presented to
IX Congres International du Verre
September, 1971

ABSTRACT

Electrical and Magnetic Property Changes During Devitrification

KINSER, D. L., WILSON, L. K., FRIEBELE, E. J.
AND DOZIER, A. W.*

Electrical conductivity and electron spin resonance (ESR) measurements were conducted on 55 mole % FeO-45 mole % P_2O_5 glasses with varying Fe^{3+}/Fe and thermal heat treatments. The DC conductivity and ESR linewidth observations exhibit breaks at about 75°C. This correlation is interpreted to indicate mechanism coupling between the two processes. The magnitude of the magnetic resonance was observed to be much smaller than that expected for the amount of Fe^{3+} present. This indicated that the spins are almost all antiferromagnetically ordered, hence the atomic structure is partially ordered to accomodate magnetic ordering. This also indicates that the short range order in the glass is considerably higher than a random phosphate network with a high modifier content would allow. Dielectric behavior was interpreted on the basis of Maxwell-Wagner-Sillars heterogeneous dielectric behavior.

Paper Submitted to the Journal of the American Ceramic Society
Do not quote or refer to contents without authors' permission.

CORRELATIONS BETWEEN STRUCTURE AND ELECTRICAL PROPERTIES IN A 55a/o FeO--45a/o P_2O_5 GLASS

A. W. Dozier*, L. K. Wilson†, E. J. Friebele*,
and D. L. Kinser†

School of Engineering
Vanderbilt University
Nashville, Tennessee
37203

The A.C. and D.C. characteristics of a 55a/o FeO--45a/o P_2O_5 glass were measured as a function of heat treatment time at 600°C and Fe^{3+}/Fe^{Tot} ratio. A correlation was established between the behavior of the D.C. resistivity vs. 1/T with varying heat treatment times and the appearance of a high and lower frequency dispersion in the tan $\delta_{A.C.}$ vs. frequency measurements. A theory explaining this correlation is proposed and evidence in support of this theory obtained from Guinier DeWolff powder camera data.

---

*Graduate Assistant, Vanderbilt University School of Engineering

†Associate Professor, Vanderbilt University School of Engineering

INTRODUCTION

The study of A.C. phenomena in semiconducting glasses is a relatively new area. The first works appeared around 1965, and were concerned with conductivity as a function of frequency, and dielectric loss observations.[1,2,3] One of these, by Hansen and Splann[2], plotted the dielectric loss parameter as a function of frequency for a 55a/o FeO--45a/o P_2O_5 glass. Loss peaks appeared in this data, and were attributed to a resonance phenomena associated with charge carriers moving between transition metal cation sites on the amorphous lattice, i.e., Schmid's small polaron conduction mechanism for amorphous semiconductors. Hansen's specimens were annealed at relatively high temperatures (450-500°C), and these loss peaks were attributed to an inhomogeneous dielectric, resulting in a loss of the Maxwell-Wagner-Sillars type, by Kinser.[4] Transmission electron microscopy was used to support Kinser's observations. Similar phenomena had been observed in other amorphous systems earlier.[5,6]

The purpose and scope of this paper is to examine the A.C. and D.C. properties of a 55a/o FeO--45a/o P_2O_5 glass as a function of heat treatment time at elevated temperatures, and as a function of varying Fe^{3+}/Fe^{Tot} ratios. These measurements were correlated with the appearances of crystalline phases in Guinier de Wolff powder camera data. A study of D.C. and A.C. properties and density as a function of quenching rate is also included.

EXPERIMENTAL PROCEDURE

Specimens were made by melting 300 gm. batches of reagent quality material in silica crucibles for one hour at 1300°C. The melting time was measured from the last addition to the crucible. Thirty minutes were required to melt the entire batch. Varying Fe^{3+}/Fe^{Tot} ratios were obtained by adding different amounts of dextrose to the melt. The pouring sequence of the specimens from the melt was recorded, and the specimens were divided sequentially into groups of about five each. The time from the first specimen poured to the last was about 40 minutes.

Two specimen configurations were used. One type was produced by a plunger and die configuration, which yielded cylindrical specimens 1.7 cm. in diameter and from .4 to .5 cm. in thickness. Specimens about .3 cm. in thickness and from 2.5 to 5.0 cm. in diameter were obtained by quenching between two copper plates 8 cm. x 15 cm. x 1.5 cm. in the other method. The quenching rate was varied in both cases by cooling the molds to 77°K, 25°C and 300°C preheat. After casting, the specimens were strain annealed at 300°C for one hour.

Both x-ray and electrical specimens used in the experiment were from the middle group of each batch. Titrations were run on specimens in the first and last group poured in each melt, as well as specimens in the middle group, for melts in which the plunger and die configuration were used. This was not necessary in the case where copper plates were used, due to the fact that the specimens were large enough to make an electrical specimen and have enough material left over for x-ray specimens and a titration. Titrations were also run as a function of heat treatment time. The titration was made in two steps, one to determine Fe^{2+}, the other to determine Fe^{Tot}. The possible error in the

Fe^{3+}/Fe^{Tot} ratio was determined to be ±.043. From these values, the Fe^{3+}/Fe^{Tot} ratios could be determined. This ratio did not vary more than the possible error in specimens poured first in the melt, and those poured last. Both steps of the titration were carried out under a nitrogen atmosphere, and in both steps approximately .5 gm. of specimen was dissolved in concentrated HCl. In the Fe^{Tot} titration, all Fe ions were first reduced to the Fe^{2+} state using stannous chloride. Excess Sn^{2+} ions interfere with the titration and were, therefore, displaced by adding mercuric chloride to the solution. The excess Hg^{2+} ions formed an insoluble precipitate, Hg_2Cl_2, in the HCl solution. The titration for Fe^{2+} was then performed using diphenylamine sulfonic acid as an indicator and potassium dichromate as a titrant.

Electrical specimens were made by evaporating gold electrodes in a guard ring configuration on the specimen, and then annealing for one hour at 300°C to allow diffusion bonding to take place. D.C. measurements were made using conventional guarded techniques. A.C. measurements were made in the audio frequency range using a Wayne Kerr B221 audio bridge in conjunction with a Hewlett-Packard 615B oscillator. The measurements were made in the radio frequency range using a Wayne Kerr B601 radio frequency bridge with an external null detector.

Guinier and DeWolff powder camera specimens were made by taking chips of the various barches, heat treating them, and grinding them in a porcelain mortar. Exposures were made for 24 hours using MoKα radiation.

EXPERIMENTAL RESULTS

Table 1 gives melt number, specimen thickness, density, Fe^{3+}/Fe^{Tot} ratio and quenching specifications for all specimens used in this experiment. Figures 1-3 show the D.C. $\log_{10}$ resistivity vs. 1/T data as a function of heat treating time for specimens with Fe^{3+}/Fe^{Tot} ratios of .31, .44, and .76, respectively. The behavior is typical of that expected from an amorphous semiconductor, and none of the specimens exhibited a time dependent variation of resistivity. The resistivity was extrapolated to 200°C and plotted with that of Hansen and Splann[2] in Figure 4. The tan δ_{AC} vs. frequency plots for specimens 4, 6, and 9 is plotted in Figures 5-7. All A.C. measurements were made at approximately 130°C. Notice that a peak around $f = 4.0 \times 10^3$ Hz appears in the as-cast data for specimen 6, whereas there are no corresponding peaks in the as-cast data for specimens 4 and 9. This specimen (number 6) was prepared using the plunger and die at 77°K. A melt of the same Fe^{3+}/Fe^{Tot} ratio as specimen 6 was prepared and copper blocks cooled to 77°K were used to make specimens in this case. The A.C. and D.C. data for a specimen from this melt (number 14) appears in Figures 8 and 9. Notice that the magnitude of the tan δ_{AC} vs. frequency peak for specimen 14 is greater than that for specimen 6, although the agreement between the D.C. $\log_{10}$ resistivity vs. 1/T plots for these specimens is good.

Table 3 presents the results of the Guinier DeWolff powder camera data for the melts as a function of heat treating time and Fe^{3+}/Fe^{Tot} ratio. Although the intensity of some lines increased with heat treatment time in some cases and decreased in others, quantitative analysis

of relative amounts of phases present was difficult, due to overlap of the x-ray spectra of these phases. As a result, precise analysis of crystalline phases precipitating out with extended heat treatments was difficult, but lines were detected in the spectra which have been tentatively attributed to those phases given in Table II. As can be seen from the table, several crystalline phases are detected in heat treatments of one hour at 600°C. The phases present vary with Fe^{3+}/Fe^{Tot} ratio.

The effect of different quenching rates on the D.C. and A.C. data for a typical melt (Fe^{3+}/Fe^{Tot} = .71) were also examined. The results are shown in Figures 10 and 11. Figure 10 contains the as-cast $\log_{10}$resistivity vs. 1/T data for specimens 11, 12 and 13, which were quenched with copper blocks cooled to -196°C, 25°C and 300°C preheat, respectively. Figure 11 contains tan δ_{AC} vs. frequency for these specimens.

DISCUSSION OF RESULTS

X-Ray Data

As can be seen in Table II, the first crystalline phase which precipitates out for all Fe^{3+}/Fe^{Tot} ratios studied in this experiment was $FePO_4$, or Iron (III) Phosphate, an Fe^{3+} rich phase. Although ratios of .31 and .44 yielded lines which were attributed to two or three other phases, the relative intensities indicated that $FePO_4$ precipitated out first in all cases. For the same exposure time, more lines appeared after one hour heat treatments as the Fe^{3+}/Fe^{Tot} ratio decreased, indi-

cating that the phases are growing more rapidly, since the volume fraction in a given volume of material increases to the point where the weaker reflections appear.

The intensity of lines identified as $FePO_4$ remained the same with increased heat treatment time for Fe^{3+}/Fe^{Tot} ratios of .44 and .76, and decreased slightly for the .31 ratio. This distinction is marginal at best. The indication is that the amount of $FePO_4$ does not change significantly with heat treating times up to 10 hours, the maximum heat treatment time used in this experiment. At later heat treatment times, other lines appear and increase in intensity, indicating that other phases are precipitating out, and the volume fraction is increasing with heat treatment time.

Overall conclusions from the powder camera data indicate that the same Fe^{3+} rich pahse precipitates out first for all Fe^{3+}/Fe^{Tot} ratios. Other phases which are Fe^{2+} rich appear later. If the phases which precipitate out do not tie up all Fe cations in the glassy matrix, the overall indication of this behavior would be an initial decrease in the Fe^{3+}/Fe^{Tot} ratio of the glassy matrix, with a subsequent rise in this ratio at later heat treatment times.

D.C. Data

The D.C. $\log_{10}$resistivity vs. 1/T data for specimens with the same Fe^{3+}/Fe^{Tot} ratios indicates that this type of behavior does occur. This can be illustrated by looking at Figure 4. If a specimen has a high Fe^{3+}/Fe^{Tot} ratio in the as-case state, i.e., no crystals present on the amorphous matrix, and was then heat treated so that the Fe^{3+}/Fe^{Tot}

ratio of the matrix would drop, due to crystallization of an Fe^{3+} rich phase, an overall drop in resistivity as a function of 1/T should occur. This can be seen to occur in Figure 3. If, at a later time, a crystalline phase precipitated out which tied up Fe^{2+} ions, the Fe^{3+}/Fe^{Tot} ratio of the matrix would be expected to rise. This would result in a subsequent rise in resistivity. As can be seen from Figure 3, this behavior does occur. After 2 hours heat treatment at 600°C the resistivity rises.

From Figure 4, it can be seen that for a low Fe^{3+}/Fe^{Tot} ratio the opposite behavior would be observed. In other words, if the Fe^{3+}/Fe^{Tot} ratio initially drops, the resistivity of the matrix would rise. At a later time, when Fe^{2+} ions are tied up and the ratio begins to rise, the overall resistivity of the matrix would drop again. As can be seen from Figure 1, this type of behavior is observed for the Fe^{3+}/Fe^{Tot} = .31 specimen. The resistivity of the matrix rises after 1 hr. at 600°C, and subsequently drops after the 2 hr. heat treatment. However, it then rises after the 5 hr. treatment and drops again below the 2 hr. value. This could be the result of other crystalline phases becoming dominant. As can be seen in Table II, more than two phases are detected on the glassy matrix. However, analysis of relative amounts of phases is almost impossible, as has been pointed out before. A second possibility is the creation of a contiguous path of crystals from one electrode to another. Several specimens were broken after heat treatments at 600°C and a dense layer of crystal nuclei could be seen with the naked eye around the surface of the specimen. If contiguous crystals are responsible, it would appear that the drop in resistivity would be much greater than that observed, however. This latter effect was observed by M. O'Horo

and R. Steinitz[7] in a similar experiment with an alumino-borosilicate with 12 a/o Fe_2O_3. A similar effect was observed for the Fe^{3+}/Fe^{Tot} = .44 specimen as can be seen in Figure 2. However, the overall change in resistivity as a function of heat treatment time is much smaller than that observed for the specimens in Figures 1 and 3. This is easily explained by the slope of the resistivity at constant temperature vs. Fe^{3+}/Fe^{Tot} plot in Figure 4. As can be seen in Figure 4, the slope at a ratio of .44 on Hansen's plot is less than that at the extreme values of Fe^{3+}/Fe^{Tot} ratio. This would result in an overall change which would be much smaller for a similar change in ratios for all specimens.

A.C. Data

The growth of the crystalline phases is supported by the A.C. tan δ_{AC} vs. frequency for these specimens. If a higher conducting crystalline phase grows in a lower conducting matrix, a dispersion will occur in the tan δ_{AC} vs. frequency data in correspondnece with a Maxwell-Wagner-Sillars type of inhomogeneous loss mechanism. The presence of different phases of differing conductivity or morphology would result in a dispersion which would occur at different frequencies for the different phases present.

The A.C. data for the Fe^{3+}/Fe^{Tot} = .76 specimen can be seen in Figure 7. As can be seen from the figure, no dispersions appear in the as-cast data. After 1 hr. heat treatment at 600°C, a dispersion appears at around 4.0×10^4 Hz with a slight inflection at approximately 10^4 Hz. With subsequent heat treatment the low frequency inflection develops into a dispersion and, at 10 hrs., the magnitude of both dis-

persions has increased. As can be seen from the Guinier-DeWolff powder camera data, only two phases were detected at extended heat treatment times for this Fe^{3+}/Fe^{Tot} ratio specimen. It seems reasonable that an explanation of the two peak phenomena lies in the nucleation and development of two crystalline phases in the glassy matrix. However, as can be seen from Table II, no crystalline phases were detected in the powder camera data for this specimen after a one hour heat treatment at 600°C. This apparent discrepancy is best explained by the method in which x-ray specimens were obtained. Table I indicates that the specimens for this melt were made using the plunger and die mold configuration. The powder camera specimens were obtained from pieces which broke off of the buttons during the strain anneal at 300°C. These pieces, which came from the edges of the cylindrical specimens, had a different thermal history than the bulk of the specimen. As a result, it is probable that the center of the specimen had crystal nuclei present after one hour, whereas the more rapidly quenched x-ray specimen did not.

A less defined dispersion behavior can be seen in the $Fe^{3+}/Fe^{Tot} = .31$ specimen in Figure 5. It should be noted that dispersions appear in the as-cast A.C. data, although this is not the case for the powder camera data. A reasonable explanation is again found in the difference in thermal history of the bulk electrical specimen and the powder camera specimen since, as can be seen in Table I, the specimen was prepared using the plunger and die configuration mold, which made a rapid quenching rate difficult. As a control, another specimen with the same Fe^{3+}/Fe^{Tot} ratio was prepared using copper plates cooled to 77°K. As

can be seen in Figure 8, the D.C. plot was colinear in the high temperature region, although the low temperature region is difficult to compare due to a smaller number of corresponding points. The A.C. data can be seen in Figure 9. The as-cast plot of tan δ_{AC} vs. frequency reveals no dispersions, although the magnitude of the plot is much greater than the same plot for the less rapidly quenched specimen in Figure 5. A similar effect of quenching rate on A.C. data was observed by Charles.[5] It should be noted that the peaks which develop with heat treatment are not as well-defined as those in Figure 7, and are asymmetrical. This is probably due to the overlap of the dispersions from the other phases present after heat treatment, as can be seen in Table II.

The analysis of the data for specimens of $Fe^{3+}/Fe^{Tot} = .44$ was complicated due to the fact that they had a tendency to break even with the slightest heat treatment at elevated temperatures. At best the A.C. plots for specimen 9 indicated that there were essentially no loss peaks present. According to the theory developed here, this leaves two possibilities pertaining to the nucleation of crystals in these specimens. Either there were no crystals present after heat treatments of up to two hours, or the crystal nuclei were so large that dispersions would not appear in the frequency range examined. The latter possibility is the most plausible, since the crystallites could be seen with the naked eye in the specimens of this Fe^{3+}/Fe^{Tot} ratio which fractured due to residual strain.

Quenching Experiment

An experiment was run on a Fe^{3+}/Fe^{Tot} = .71 melt to detmine the effect of quenching rate on density and electrical properties. Specimens 11, 12, and 13 were quenched using copper blocks cooled to -196°C, 25°C, and 300°C, respectively. The data from this experiment can be seen in Figures 10 and 11. No dispersions appear in the A.C. data of any of the specimens. It can, therefore, be concluded that the quenching rate on the low Fe^{3+}/Fe^{Tot} specimens is not as critical to glass formation as the high ratio melts. As ahs been mentioned before, the same result was observed from the Guinier-DeWolff powder camera data. Also, as can be seen from Figure 10, the resistivity increases with decreasing quenching rate. From Table I, it can be seen that the density of these specimens decreases with decreasing quenching rate. In other words, the separation between adjacent Fe cations becomes larger with increased or more rapid quenching rates. This can be correlated with the corresponding increase in resistivity.

CONCLUSIONS

1. D.C. data for the various Fe^{3+}/Fe^{Tot} ratios behaves in a manner which indicates the growth of several different crystalline p ses when the specimens are heat treated for varying times at 600°C.

2. Double peaks appear in the tan $\delta_{A.C.}$ vs. frequency data which can be attributed to different crystalline phases growing in the glassy matrix.

3. These dielectric loss peaks appear simultaneously with crystalline phases in the specimens, as indicated by the Guinier-DeWolff powder camera data.

4. The ease of homogeneous glass formation varies with the Fe^{3+}/Fe^{Tot} composition of the melt. As a result the effect of different quenching rates on the formation of a homogeneous glass is not as critical for the low Fe^{3+}/Fe^{Tot} ratio, as the high ratio.

5. An increased, or more rapid quenching rate decreases the density of the specimens, thereby increasing the separation of the Fe ions and causing a rise in the resistivity of the specimen.

ACKNOWLEDGMENTS

The authors gratefully acknowledge the financial support provided by Project Themis under contract # DAAD05-69-C-0043, and ARO-D under contract # DAHC04-70-C-0046.

REFERENCES

[1] L. L. Hench and D. L. Jenkins, "A. C. Conductivity of a Glass Semiductor," Phys. Stat. Sol. 20, 327 (1967).

[2] K. W. Hansen and Mary T. Splann, "Semiconduction in Iron Phosphate Glasses," J. Elect. Soc. 112, 994 (1965).

[3] K. W. Hansen and Mary T. Splann, "Dielectric Properties of Semiconducting Iron Phosphate Glasses," J. Elect. Soc. 113, 895 (1966).

[4] D. L. Kinser, "Structure and Electrical Properties of FeO-P_2O_5 Glasses," J. Elect. Soc. 117, 546 (1970).

[5] R. J. Charles, " Some Structural and Electrical Properties of Lithium Silicate Glasses," J. Am. Cer. Soc. 46, 235 (1963).

[6] D. L. Kinser and L. L. Hench, "Effect of a Metastable Precipitate on the Electrical Properties of an Li_2O-SiO_2 Glass," J. Am. Cer. Soc. 51, 445 (1968).

[7] M. O'Horo and R. Steinitz, "Characterization of Devitrification of an Iron-Containing Glass by Electrical and Magnetic Properties," Mat. Res. Bull. 3, 117 (1968).

LIST OF TABLES

TABLE I

PERTINENT DATA ON ELECTRICAL SPECIMENS USED

ALL SPECIMENS - 55a/o FeO--45a/o P_2O_5 COMPOSITION

Specimen Number	Melt Number	Density (gm/cm^3)	Fe^{3+}/Fe^{Tot}	Comments
4	1		.755	Ambient plunger and die mold
6	2		.306	Liquid nitrogen cooled plunger and die mold configuration.
9	3		.440	Ambient plunger and die mold
11	4	3.03032	.710	Liquid nitrogen cooled plunger and die mold.
12	4	3.03157	.710	Ambient plunger and die mold
13	4	3.03249	.710	300°C preheat plunger and die
14	5		.306	Liquid nitrogen cooled copper blocks

TABLE II

PHASE OBSERVED IN X-RAY ANALYSIS

H. T. Time @ 600°C	Fe^{3+}/Fe^{Tot}		
	.31	.44	.76
1 hr.	FeO Fe_2O_3 Fe_3O_4 $FePO_4$	$FePO_4$	None
2 hr.	No Data Taken	$FePO_4$ Fe_3O_4	$FePO_4$
10 hr.	$FePO_4$ (I_R decreased) Fe_3O_4 Fe_2O_3 FeO	$FePO_4$ Fe_3O_4 Fe_2O_3 FeO	$FePO_4$ Fe_3O_4

LIST OF FIGURES

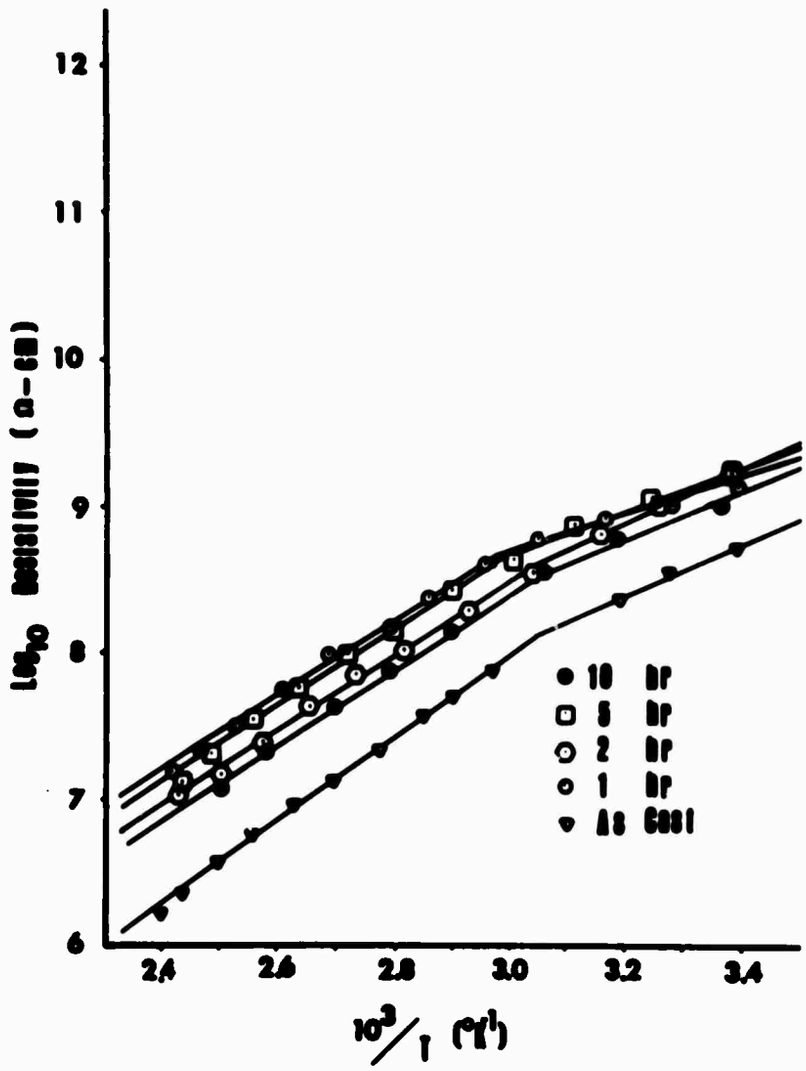

Figure 1. Log_{10} resistivity vs. 1/T as a function of heat treatment time at 600°C for specimen 6, Fe^{3+}/Fe^{Tot} = .31.

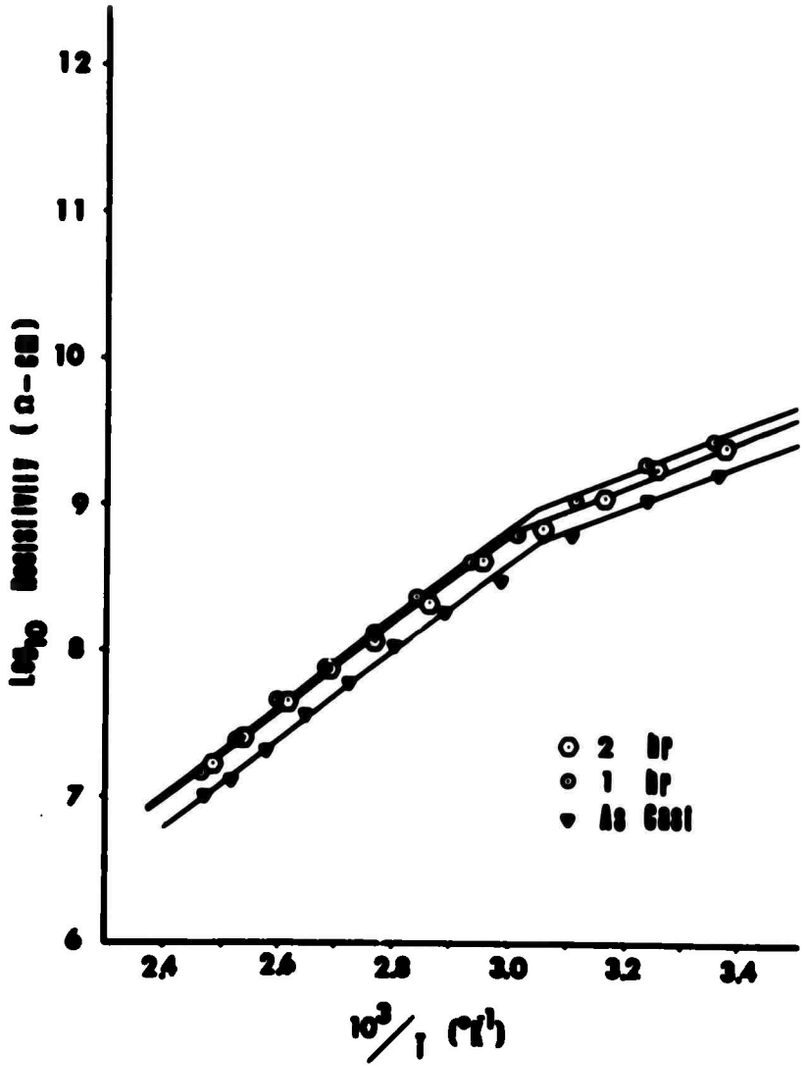

Figure 2. Log_{10} resistivity vs. 1/T as a function of heat treatment time at 600°C for specimen 9, Fe^{3+}/Fe^{Tot} = .44.

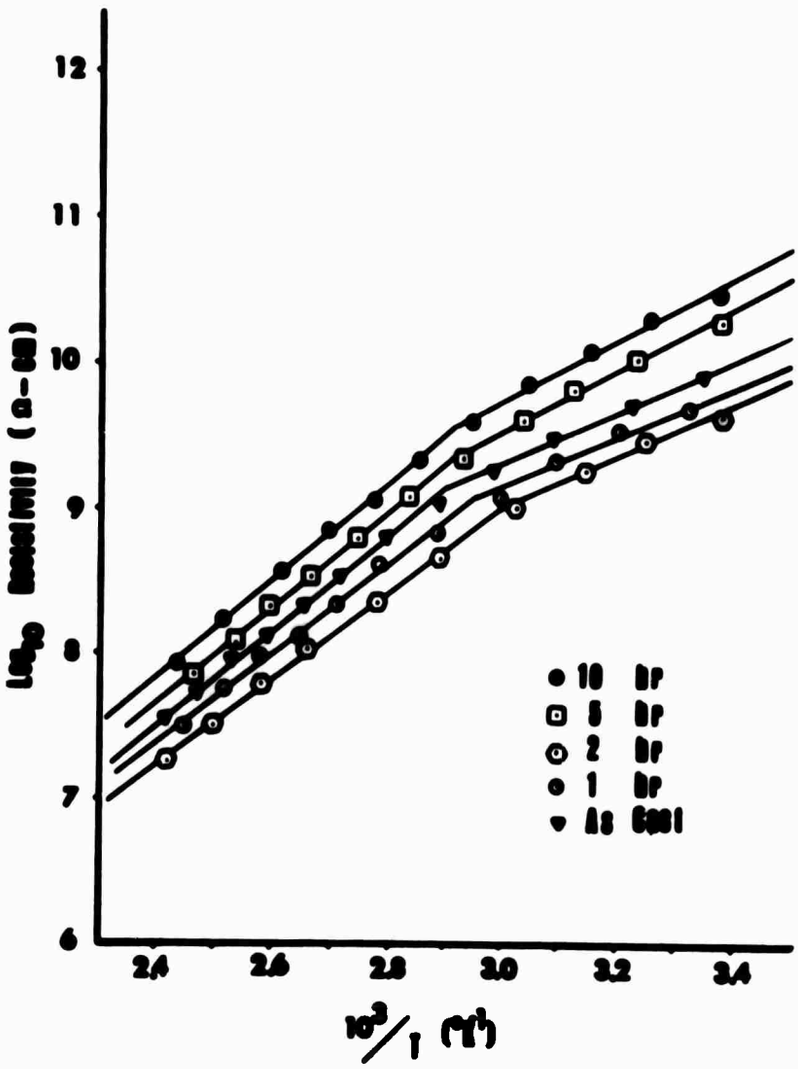

Figure 3. Log_{10} resistivity vs. 1/T as a function of heat treatment time at 600°C for specimen 4, Fe^{3+}/Fe^{Tot} = .76.

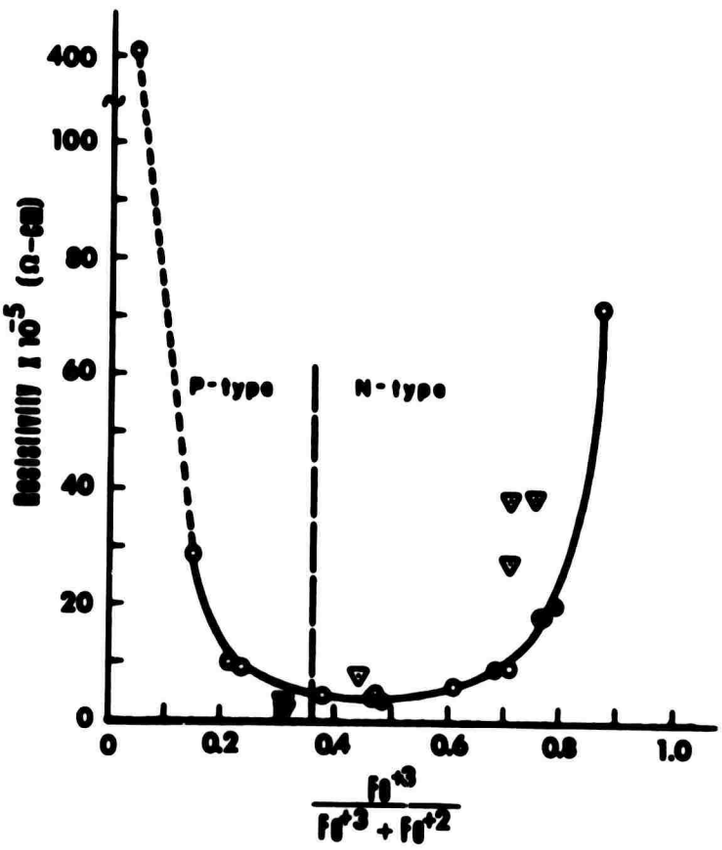

Figure 4. Extrapolated resistivity at 200°C vs. Fe^{3+}/Fe^{Tot}. The data of Hansen, ● ○, is shown along with the data collected in this experiment ▽ . Hansen's data for a 55a/o FeO--45a/o P_2O_5 glass.

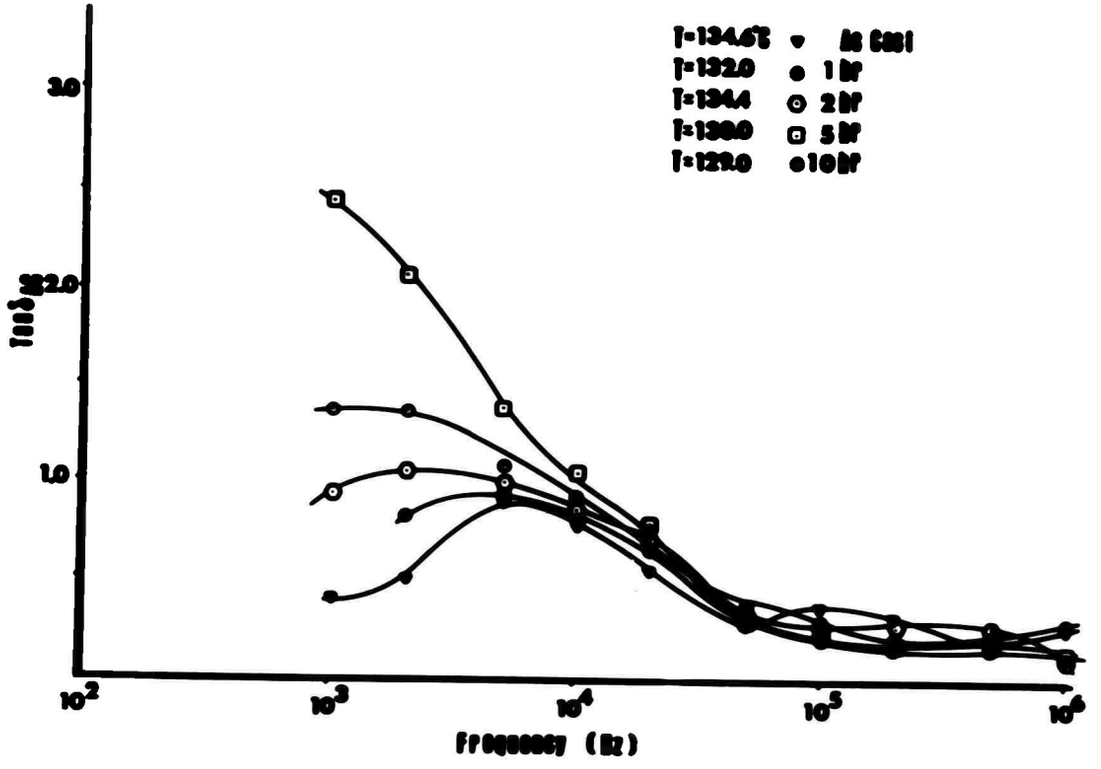

Figure 5. Tan δ_{AC} vs. frequency for specimen 6, Fe^{3+}/Fe^{Tot} = .31, as a function of heat treatment time at 600°C.

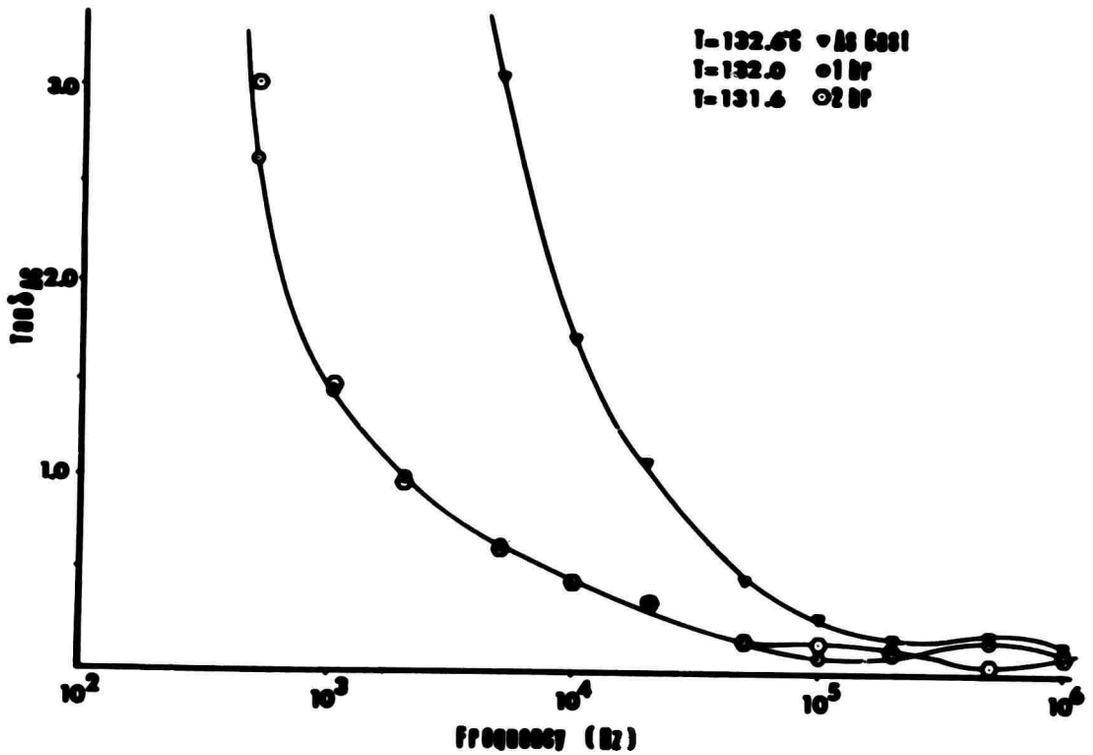

Figure 6. Tan δ_{AC} vs. frequency for specimen 9, Fe^{3+}/Fe^{Tot} = .44, as a function of heat treatment time at 600°C.

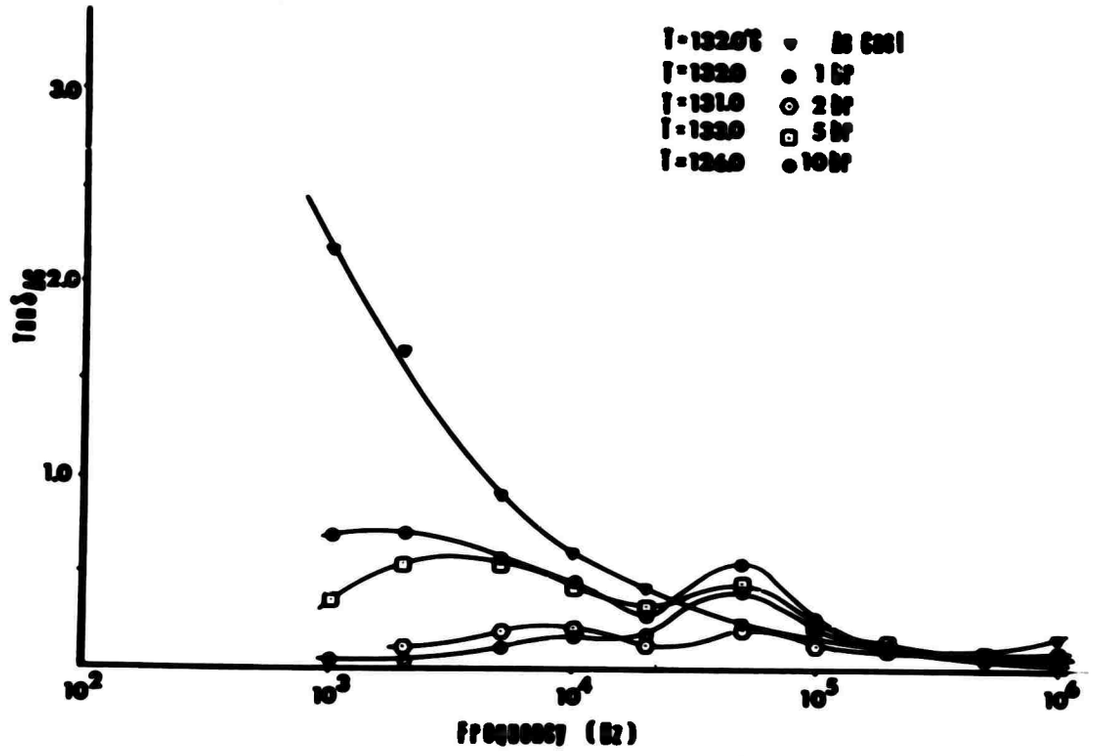

Figure 7. Tan δ_{AC} vs. frequency for specimen 4, Fe^{3+}/Fe^{Tot} = .76, as a function of heat treatment time at 600°C.

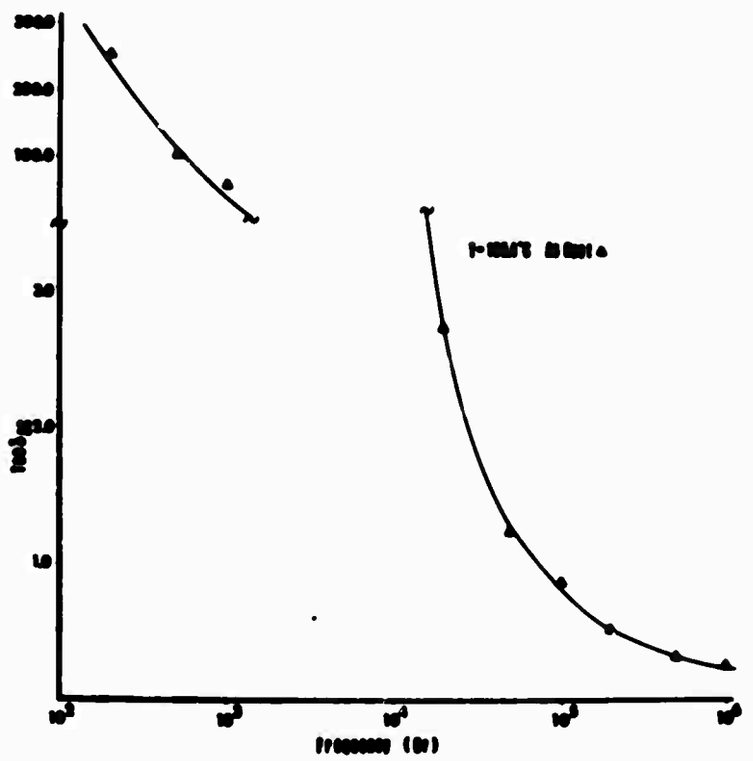

Figure 9. Tan δ_{AC} vs. frequency for specimen 14, Fe^{3+}/Fe^{Tot} = .31, as a function of heat treatment time at 600°C.

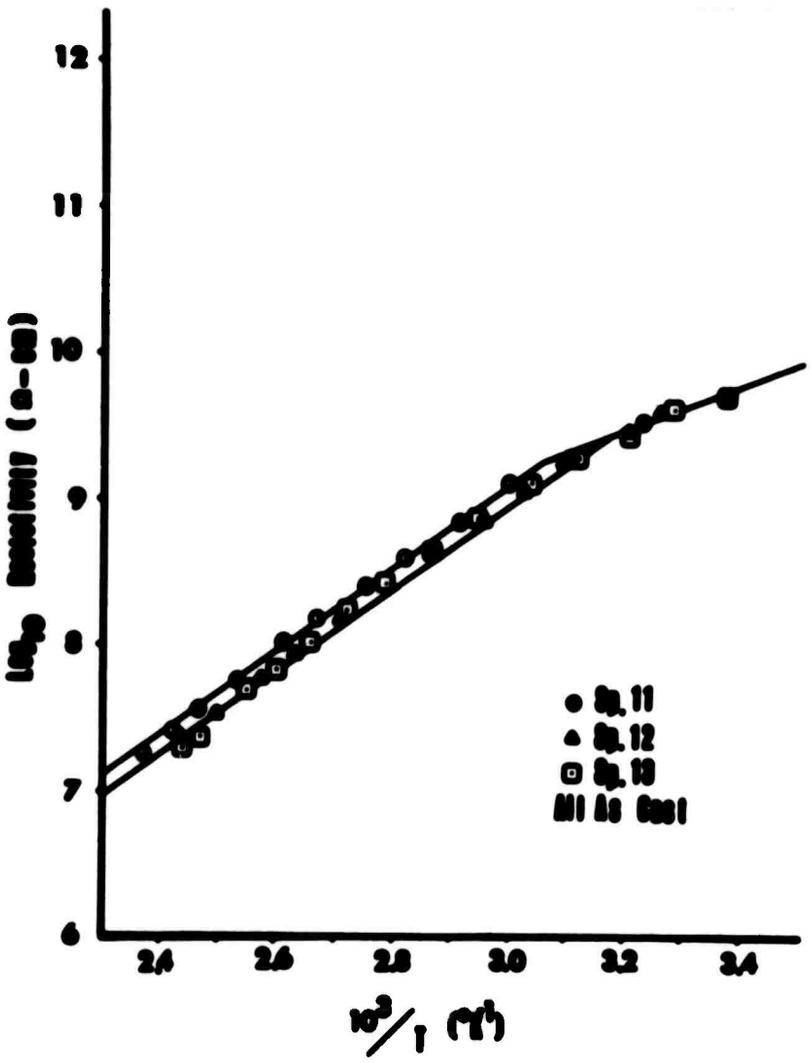

Figure 10. Log_{10} resistivity vs. 1/T as a function of heat treatment time at 600°C for specimens 11, 12, and 13, Fe^{3+}/Fe^{Tot} = .710.

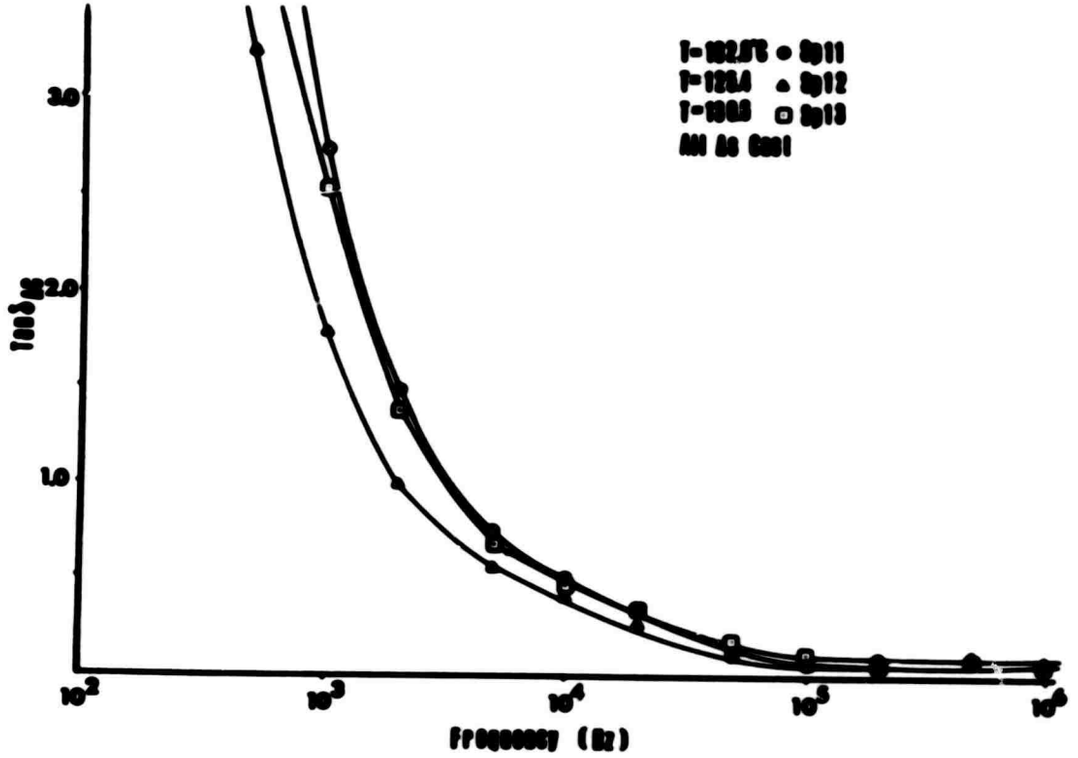

Figure 11. Tan δ_{AC} vs. frequency for specimens 11, 12, and 13, Fe^{3+}/Fe^{Tot} = .71, as a function of heat treatment time at 600°C.

Note: This is a draft of a paper being submitted for publication. Contents of this paper should not be quoted nor referred to without permission of the authors.

MAGNETIC BEHAVIOR AND MICROSTRUCTURE OF VANADIUM-PHOSPHATE GLASSES

E. J. Friebele, Graduate Student
Department of Electrical Engineering

L. K. Wilson, Associate Professor
Department of Electrical Engineering

D. L. Kinser, Associate Professor
Department of Materials Science Engineering

School of Engineering
Vanderbilt University
Nashville, Tennessee
June, 1971

This paper was originally presented at the 73rd Annual Meeting of the American Ceramic Society in Chicago, Illinois, April 27, 1971. (14-E-71)

ABSTRACT

The magnetic properties and microstructure of the vanadium phosphate glass system over the composition range 60-90 mole % V_2O_5 were investigated in order to study the magnetic ordering in the glass and to study the effect of the microstructure upon its magnetic properties. It was determined that direct antiferromagnetic coupling between V^{4+} ions in the glassy matrix existed with a transition temperature near -70°C. It was also determined that as-cast glasses with a high concentration of V_2O_5 separated into two glassy phases. This separation caused an increase in ESR linewidth due to inhomogeneity broadening. The separation, which concentrated the vanadium ions in a vanadium-rich phase, caused a hysteresis in the ESR line intensity vs temperature plot at the transition temperature. Reduction of the vanadium ions by addition of dextrose to the melt enhanced phase separation and resulted in weak antiferromagnetic transitions at +70 and -120°C, the Neél temperatures of VO_2 and V_2O_3, respectively.

MAGNETIC BEHAVIOR AND MICROSTRUCTURE OF VANADIUM-PHOSPHATE GLASSES

I. INTRODUCTION

The vanadium-phosphate glass system has been the subject of investigation since 1868 (1), and recently, extensive studies of the electrical conductivity of this system have been made in an attempt to understand the electronic conduction mechanism in transition metal oxide glasses (2). In addition, the magnetic behavior of these glasses has been studied in order to elucidate the magnetic structure and to correlate this structure with behavior observed in conductivity measurements (3-11). Throughout the literature, however, there is considerable disagreement over the magnetic behavior of the V_2O_5-P_2O_5 glass system. There have been several reports of phase separation in this system (12-14), and since none of the previous magnetic studies have considered the effect of separation on the magnetic properties, this research was undertaken.

The present work reports an investigation of the magnetic ordering in the glass, correlations between magnetic transitions in the glass and known transitions in the various vanadium oxides, and the first reported study of the effect of the microstructure on the magnetic properties of vanadium-phosphate glasses.

II. EXPERIMENTAL

The glass samples were prepared by melting a physical mixture of V_2O_5 in silica crucibles in air for one hour at 1100°C. Each melt was then quenched to room temperature on copper plates. Six different compositions were studied: 60-40, 65-35, 70-30, 75-25, 80-20, and 90-10 mole percent V_2O_5-P_2O_5. In order to obtain samples with increased concentrations of the lower valence vanadium ions, dextrose was added to one batch each of the 65-35 and 80-20 glasses.

MAGNETIC BEHAVIOR AND MICROSTRUCTURE OF VANADIUM-PHOSPHATE GLASSES

I. INTRODUCTION

The vanadium-phosphate glass system has been the subject of investigation since 1868 (1), and recently, extensive studies of the electrical conductivity of this system have been made in an attempt to understand the electronic conduction mechanism in transition metal oxide glasses (2). In addition, the magnetic behavior of these glasses has been studied in order to elucidate the magnetic structure and to correlate this structure with behavior observed in conductivity measurements (3-11). Throughout the literature, however, there is considerable disagreement over the magnetic behavior of the V_2O_5-P_2O_5 glass system. There have been several reports of phase separation in this system (12-14), and since none of the previous magnetic studies have considered the effect of separation on the magnetic properties, this research was undertaken.

The present work reports an investigation of the magnetic ordering in the glass, correlations between magnetic transitions in the glass and known transitions in the various vanadium oxides, and the first reported study of the effect of the microstructure on the magnetic properties of vanadium-phosphate glasses.

II. EXPERIMENTAL

The glass samples were prepared by melting a physical mixture of V_2O_5 in silica crucibles in air for one hour at 1100°C. Each melt was then quenched to room temperature on copper plates. Six different compositions were studied: 60-40, 65-35, 70-30, 75-25, 80-20, and 90-10 mole percent V_2O_5-P_2O_5. In order to obtain samples with increased concentrations of the lower valence vanadium ions, dextrose was added to one batch each of the 65-35 and 80-20 glasses.

Dilatometric measurements on the glass samples showed that all glasses had a softening point near 250°C (14), and for this reason, none of the as-cast samples were annealed after quenching.

Finely powdered glass samples were examined in a vacuum Guinier-De Wolff X-ray camera using MoK_{α} radiation. This technique permits detection and identification of as little as 0.1 wt. % crystal. However, no evidence of crystallinity was found in any of the samples of the as-cast or heat-treated glasses.

ESR measurements were made on a Varian V4500 spectrometer at 9 GHz. Variations in sample temperature were obtained through use of a Varian V4540 variable temperature apparatus and a hydrogen Cryotip. Magnetic field strength was determined by means of a proton spin resonance gaussmeter, and the klystron frequency was measured by a direct reading hetrodyne frequency counter.

In order to determine the spin density of each resonance line and to study the intensity of the line as a function of experiment temperature, it was necessary to calculate the area under the absorption curve, $I = \Delta H^2 h_{pp}$, where ΔH is the linewidth and h_{pp} is the peak-to-peak height of the first derivative line (15). The spin density was determined by comparison with a calibrated sample. Likewise, the normalized intensity of the ESR line was determined by dividing the intensity of the glass resonance by the intensity of a paramagnetic standard (DPPH) in order to remove the temperature dependence of the sensitivity of the spectrometer (16).

III. RESULTS

The first derivative ESR spectra of the as-cast glass samples consists of a singlet centered at $g' = 1.96 \pm 0.005$. The linewidths of the room temperature spectra of the various compositions are shown in Figure 1. The linewidth

and g' value of each sample remained constant throughout the temperature range studied. No hyperfine structure was found on any of the resonances of the glasses.

To further investigate the magnetic structure of the system, variable temperature ESR and magnetic susceptibility measurements were made. ESR results from representative samples are shown in Figures 2-4. It is apparent from the ESR data that there is a weak antiferromagnetic transition near -70°C. Phase separated samples show a hysteresis in the intensity at this point. It may also be noted from Figures 2 and 3 that reduction of the vanadium ions by addition of dextrose to the melt causes extremely weak transitions near +70 and -120°C.

Representative electron micrographs of two of the as-cast glasses are shown in Figures 5 and 6. The results of the microscopy studies show increasing phase separation and growth of a second glassy phase as the vanadium content is increased. Although no structure was found in the 60-40 glass, it can be seen that there is a small volume fraction of the separated phase in the 65-35 glass and a much larger volume fraction in the 90-10 glass. As shown in Figure 7, heat treatment of the glasses for one hour at 300°C leads to further separation of the second phase. The effect of the heat-treatment is especially apparent upon comparison of Figures 5 and 7. Addition of dextrose to the melt in order to reduce the V^{5+} ions also enhances the separation (14). The ease with which the separation occurs and the difficulty of producing unseparated samples containing high vanadium concentrations clearly indicates the presence of a metastable immiscibility gap in the system. The resulting separation has a definite effect on the magnetic properties of the glasses.

IV. DISCUSSION

Figure 8 is a plot of the ratio of the concentration of V^{4+} ions to V^{5+} ions (n_4/n_5) as a function of glass composition as determined for the glasses studied by the present authors, MacKenzie (17), and Landsberger and Bray (5). It is interesting to note the close agreement between the interpolated wet chemistry data of MacKenzie and the results of the ESR studies. MacKenzie's chemistry technique results in a ratio which is actually the ratio of all reduced ions (V^{2+} V^{3+}, and V^{4+}) to V^{5+}, whereas the value determined from ESR data is actually a ratio of paramagnetic ions (V^{2+} and V^{4+}) to nonparamagnetic ones (V^{3+} and V^{5+}). The agreement indicates that the concentration of V^{2+} and V^{3+} in the unreduced glasses is extremely small.

In spite of the fact that ^{51}V, which is 99.75% naturally abundant, has a nuclear spin of 7/2, no hyperfine structure was observed in the spectra of the as-cast glasses. Hyperfine structure has been observed in alkali borate, silicate and phosphate glasses containing 5 wt. % vanadium by Bogolomova, Lazukin and Petrovykh (18). No hyperfine structure was observed in semiconducting vanadium-phosphate glasses containing more than 40 mole % V_2O_5 by Landsberger and Bray (5), or by Bogolomova, et al. (9). In contrast, Nagiev (6) and Lynch, et al. (7) reported hyperfine structure in 90-10 and 80-20 mole % V_2O_5-P_2O_5 glasses, respectively. However, neither of the above investigators reported any X-ray analysis of their glasses, and Lynch found hyperfine only in a sample which had been melted under an oxygen atmosphere. It appears probable that their glasses were partially devitrified.

The lack of hyperfine structure in the ESR spectra of the glass samples is evidence that the exchange term in the spin Hamiltonian completely dominates the hyperfine term. Since the V^{5+} ions are diamagnetic with S = 0, and since

the concentration of V^{2+} in the unreduced glass is very small, the exchange coupling must be predominantly between V^{4+} ions. It will be shown later that this coupling is antiferromagnetic, which tends to reduce the intensity of resonance line and results in a reduction in the apparent concentration of V^{4+}. The error associated with this effect is proportional to the concentration of V^{4+} ions in the glass, and thus, the values of n_4/n_5 for the glasses with high V^{4+} content are probably too small. In addition, there is a possibility of exchange coupling between V^{4+} and V^{3+} ions in the glasses containing large concentrations of the reduced ions. Such coupling would tend to broaden the resonance line and once again result in a reduction of the value for n_4/n_5 (19).

In order to explain the increase in ESR linewidth shown in Figure 1 at the higher concentrations of V_2O_5, one must investigate the structure of the glasses. Janakirama-Rao (20) has postulated a structure for vanadium-phosphate glasses, which is similar to the structure of crystalline V_2O_5, shown in Figure 9, as determined by Bachmann, Ahmed and Barnes (21). The proposed structure consists of distorted trigonal bipyramids with a vanadium ion in octahedral coordination at the center of each pyramid. The oxygen atoms on the basal corners of the pyramid link to other pyramids so that sheets of VO_5 units evolve. In crystalline V_2O_5, these units share edges to form zigzag double chains in the [001] direction and are cross-linked along [100] to other units to form parallel sheets in the x-z plane (21). In the glasses, PO_4 tetrahedra replace the non-bridging oxygen at the apex of the pyramids, and the sheets are twisted to accomodate the PO_4 units and maintain the randomness of the glass. At higher P_2O_5 concentrations, the sheets degenerate into chains and ribbons of VO_5 pyramids which are bonded to PO_4 tetrahedra (5).

As the concentration of V_2O_5 increases, the concentration of V^{4+} ions decreases, as shown in Figure 8, and thus the exchange coupling between V^{4+} decreases. In addition, the concentration of VO_5 structural units with PO_4 tetrahedra replacing the apex oxygen decreases. Janakirama-Rao (20) has determined from infrared studies that the high charge density of the phorphorous ion attracts the V-O bonding electrons away from the bond. This weakens the bond and creates considerable site-to-site variation between the vanadium sites with and without the bonded phosphate tetrahedra. As the concentration of phosphate tetrahedra decreases, ribbons and chains of VO_5 units form into sheets, and the distortion of the sheets decreases. Since the vanadium site-to-site variation decreases, the ESR linewidth should decrease. It can be seen in Figure 1 that such is the case in glasses containing less than 75 mole % V_2O_5. However, the linewidth increases for glasses containing a higher concentration of vanadium. This behavior is opposite to the prediction of the structural model, but the explanation for this increase in linewidth at high V_2O_5 concentrations can be found upon comparison of Figures 5 and 6.

Phase separation in glasses with high vanadium content is in accord with Anderson and Compton (12), who reported spinodal decomposition in an unannealed 87.5-12.5 glass. Separation has also been detected in annealed vanadium-phosphate glasses by Hamblen, Weidl and Blair (13), and Kinser, Friebele, and Wilson (14). This phase separation of the glass results in two amorphous phases--one rich in vanadium and one rich in phosphate. Since the vanadium ions in each phase would experience completely different environments, inhomogeneity broadening would broaden the ESR lines and account for the behavior observed in Figure 1.

The exchange coupling of the vanadium ions in the glass gives rise to the transition at -70°C, which is shown in Figures 2-4. Barry (22) has shown that exchange coupling between ions of the same valence state results in a resonance of decreasing intensity below the Neél temperature. Coupling between ions of different valence states not only results in extreme broadening of the resonance line (3,19), but also results in increasing intensity below the transition temperature. Since the susceptibility data indicates that the coupling is antiferromagnetic, this coupling must be predominately between V^{4+} ions.

Landsberger and Bray (5) have argued that the local environment of a V^{4+} ion in the glass is not similar to that of crystalline VO_2, but rather to that of crystalline V_2O_5. In this model the V^{4+} ions in the vanadium-phosphate glass matrix find themselves in the distorted octahedral symmetry of the VO_5 groups rather than in the tetragonal symmetry of VO_2. Then, the change of symmetry would have the effect of increasing the V^{4+}-V^{4+} interaction distance, which would weaken the exchange and lower the transition temperature. In addition, the phosphorous ion in the bonded apex phosphate group would delocalize the V-O bonding electrons and attract the additional non-bonding electron of the V^{4+} ion. This attraction towards the phosphorous ion would also weaken the exchange and lower the transition temperature from +67°C, the Neél temperature of crystalline VO_2 determined by Goodenough (23).

The high temperature magnetic susceptibility data of all glasses studied follows a Curie Weiss law. The projected Curie temperature, θ, of the unseparated samples agrees within experimental error with the transition temperature determined from ESR measurements. This indicates that the coupling which gives rise to the antiferromagnetic transition at -70°C is the result of direct exchange between nearest neighbor V^{4+} ions, and not superexchange through the bridging oxygen atoms.

Anderson (24) has shown that in materials where superexchange is known to occur, θ/T_N is greater than one, and Owen (25) states that differences between θ and T_N are the result of next nearest neighbor and higher exchanges. Thus, we conclude that in the glass matrix, the antiferromagnetic exchange is directly between V^{4+} ions in adjoining VO_5 structural units.

Certainly, the effect of this exchange on the bulk magnetic properties of the glass is fairly weak. The room temperature mass susceptibility is on the order of 10^{-6}, (cgs units/gm) and there is only a 15% variation in resonance intensity between the transition temperature and -196°C. If we assume a homogeneous glass consisting of distorted sheets of VO_5 units, the coordination number of the exchange interaction between vanadium ions will be 4. For ribbon or chain structures, the coordination number would be less, but always greater than one (for a terminal VO_5 unit on a chain). Now, the probability of a V^{4+}-V^{4+} exchange is equal to the square of the molar concentration of V^{4+} ions. The total number of V^{4+} paired exchanges in the glass is the probability of the exchange times the total number of vanadium exchanges = PZ[V]/2, where P is the probability, Z is the coordination number, and [V] is the concentration of vanadium in the glass. In the case of the 80-20 glass, in a typical ESR sample of 100 mg., there would be approximately 10^{17} V^{4+} ions in pairs. These would easily give rise to the observed transition. In glasses which are heterogeneous, the probability of V^{4+} pairs is even higher, since much of the vanadium is concentrated in a vanadium-rich phase.

Reduction of the vanadium ions by addition of dextrose to the glass melt enhances the phase separation of the as-cast glass (14). It is apparent in Figure 2 and 3 that the magnetic properties of the glass have also been altered

by the reduction. Although the reduced glasses still have the antiferromagnetic transition at -70°C, there is evidence of hysteresis in the intensity-temperature curve at this point. Similar hysteresis has been found in crystalline systems containing more than one crystalline phase (26), and the results of the present work indicate that such a correlation may also exists in the vanadium-phosphate glass system.

The anomalous behavior of the reduced glasses at +70 and -120°C may be explained in terms of antiferromagnetic transitions in the vanadium-rich phase in the glass. Reduction of the vanadium by addition of dextrose results in an increased concentration of V^{4+}. Although prior to this study no evidence of V^{3+} has been found in vanadium-phosphate glass, it is conceivable that the reduction process could also result in a small concentration of V^{3+} (and V^{2+}) in the glass. Phase separation of the glass would then concentrate the vanadium ions in the vanadium-rich phase, and exchange coupling between the reduced ions could result. Since numerous studies have indicated that the local environment of ions in glass and in the corresponding crystal is quite similar, it is reasonable to expect that the local environment of the vanadium ions in the separated, vanadium-rich phase may closely approach that of crystalline vanadium oxide.

As has previously been mentioned, Landsberger and Bray (5) have postulated that the site symmetry of a V^{4+} ion in the glass matrix is identical to that of a V^{5+} ion, so that conduction by electron hopping can occur without structural rearrangement of the glass. However, when the phase separation takes place at elevated temperatures, the ion mobility is greater and the vanadium ions in the separated phase would attempt to surround themselves with a ligand cage similar to that experienced in crystalline vanadium oxide. Since there is a low concentration of PO_4 tetrahedra in the separated phase, the local structure of

the vanadium ions in this phase could be quite different from that in the glassy matrix of unseparated glasses. One would then expect that exchange coupling between vanadium ions of the same valence state to give rise to antiferromagnetic transitions at temperatures corresponding to the Neél temperatures of VO_2 and V_2O_3. It can be seen from Figures 2 and 3 that there is evidence of extremely weak transitions near +70°C, corresponding to the Neél temperature of +70°C for VO_2 (27) and near -120°C, corresponding to the Neél temperature of -123°C for V_2O_3 (28). Although the weak inflections in the intensity curves are well within experimental error bars, they are consistently reproducible, hence lending more credibility than the error bars would allow. In addition, Hench and Jenkins (29) have found a change from frequency-independent to frequency-dependent conductivity at +70°C. Schmid (30) has explained this in terms of a transition from a small polaronic to a tunnelling conduction mechanism.

Further verification of the existence of exchange coupling in the separated phase is found by investigating the heat-treated sample (Figure 4). Once again, there is an antiferromagnetic transition at -70°C and hysteresis at this point, but upon comparison with Figure 2, it is seen that there is a definite tailing off of the intensity at high temperatures. This is not observed in the unreduced, and unseparated glass. Apparently the V^{4+} ions in the separated phase are in local ligand environments similar to those in VO_2, such that antiferromagnetic coupling between V^{4+} ions is possible. Once again, this results in a very weak magnetic transition temperature near the Neél temperature of VO_2.

V. CONCLUSIONS

The results of the present study indicate the existence of nearest neighbor antiferromagnetic coupling between V^{4+} ions in VO_5 ligand cages in the

homogeneous glass matrix. This coupling results in a transition temperature of -70°C, which is observed in all glass samples. The reduction in transition temperature from the Neél temperature of VO_2 is apparently the result of delocalization of the bonding electrons by the bonded phosphorous and the result of the distorted octahedral site symmetry of the V^{4+} in the glassy matrix.

Attempts to reduce V^{5+} to the lower valence state ions result in phase separation of the glass and weak magnetic behavior which may be explained in terms of V^{3+}-V^{3+} and V^{4+}-V^{4+} antiferromagnetic coupling in the vanadium-rich phase. This behavior is correlated with the behavior of heat-treated glasses in which phase separation has occurred, but no reduction has taken place.

The present determination of the relative concentration of V^{4+} to V^{5+} in the as-cast glasses is in agreement with two previous studies (5,17). However, the results of electron microscopy studies indicate the necessity of structurally characterizing the glass before attempting other investigations. The extent of the phase separation and growth of the second phase increased with increasing vanadium content in the glass. The fact that phase separation was observed in rapidly cooled samples indicates the existence of a metastable immiscibility gap in the V_2O_5-P_2O_5 system (14). Certainly, this phase separation in the as-cast and heat-treated glasses and the possibility of crystallization in glasses with high vanadium content can explain the disparate observations of hyperfine structure in the ESR spectra.

VI. ACKNOWLEDGMENTS

The authors would like to thank Miss Bonnie B. Baker and Mr. James W. Berry, Jr. for their assistance in gathering experimental data and Professor H. J. Kreidl for his helpful discussion. This research was supported in part by the Army Research Office - Durham under contract number DAHCO4-70-C-0046,

REFERENCES

1. H. E. Roscoe, "Researches on Vanadium," Phil. Trans. Royal Soc. 158 [1] 1-27 (1868).

2. J. D. MacKenzie, "Semiconducting Oxide Glasses," in Modern Aspects of the Vitreous State Vol. III, pp. 126-148, J. D. MacKenzie, ed. London: Butterworth Scientific Publications, Ltd., 1960.

3. E. J. Friebele, L. K. Wilson, A. W. Dozier, D. L. Kinser," Antiferromagnetism in an Oxide Semiconducting Glass," Phys. Stat. Sol. B. 45 [1] 323-333 (1971).

4. E. J. Friebele, L. K. Wilson, D. L. Kinser, "Preliminary Property Studies of a 55-45 mole % MnO_2-P_2O_5 Glass," to be published.

5. F. R. Landsberger and P. J. Bray, "Magnetic Resonance Studies of the V_2O_5-P_2O_5 Semiconducting Class System," J. Chem. Phys. 53 [7] 2757-2768 (1970).

6. V. M. Nagiev, "An Investigation of Vanadium Phosphate Glasses by Electron Paramagnetic Resonance," Sov. Phys. Sol. State 7 [9] 2204-2206 (1966).

7. F. Lynch, M. Sayer, S. L. Segel and G. Rosenblatt, "Electron and Nuclear Magnetic Resonance in Semiconducting Phosphate Glasses," J. Appl. Phys. 42 (1971), to be published.

8. P. W. France and H. O. Hooper," Nuclear Magnetic Resonance Study of Semiconducting Vanadium Phosphate Glass," J. Phys. Chem. Sol. 31 [6] 1307-1315 (1970).

9. L. D. Bogolomova, V. N. Lazukin, and N. V. Petrovykh, "Electron Paramagnetic Resonance Study of the Mechanism of Electrical Conductivity in the Glasses of the Ternary System V_2O_5-WO_3," Sov. Phys. Doklady 12 [11] 1046-1049 (1968).

10. L. M. Imanov, V. M. Nagiev and A. A. Dzhabbarov, "Unpaired Electrons and Charge Carriers in Oxide Semiconducting Glasses Based on Vanadium and Phosphorous," Izv. Akad. Nank. azerb SSSR 4 [1] 21-24 (1969).

11. L. K. Wilson and D. L. Kinser, "Electrical Conductivity and Magnetic Resonance Correlations in Transition Metal Oxide-Phosphate Glasses," Bull. Am. Phys. Soc. 15 [11] 1371 (1970.

12. G. W. Anderson and D. W. Compton," Optical Absorption Properties of Vanadate Glasses," J. Chem. Phys. 52 [12] 6166-6174 (1970).

13. D. P. Hamblen, R. A. Weidl and G. E. Blair, "Preparation of Ceramic Semiconductors from High Vanadium Glasses," J. Am. Ceram. Soc. 46 [10] 499-504 (1963).

14. D. L. Kinser, E. J. Friebele and L. K. Wilson, "Electron Microscopy of Phase Separation in Vanadium-Phosphate Glasses," to be published.

15. R. A. Weeks, A. Chatelain, J. L. Kolopus, D. Kline, and J. G. Castle, Jr., "Magnetic Resonance Properties of Some Lunar Materials," Science 167 [3918] 704-707 (1970).

16. R. J. Landry and J. T. Fournier, "ESR and Optical Absorption Studies of Transition Metal Ions and Color Centers in Glass," Office of Naval Research, 1969.

17. J. D. MacKenzie, "Semiconducting Glasses," Tech Report 5, Contract Nonr-591 (21).

18. L. D. Bogolomova, V. N. Lazukin and N. V. Petrovykh, "Hyperfine Structure of the Electron Paramagnetic Resonance Spectra of the Vanadyl Ion in Vanadium-Containing Glass," Sov. Phys. Doklady 12 [8] 780-782 (1968).

19. J. H. Van Vleck, "The Dipole Broadening of Magnetic Resonance Lines in Crystals," Phys. Rev. 74 [9] 1168-1183 (1948).

20. Bh. V. Janakirama-Rao, "Infrared Spectra of GeO_2-P_4O_{10}-V_2O_5 Glasses and their Relation to Structure and Electronic Conduction," J. Am. Ceram. Soc. 49 [11] 605-509 (1966).

21. H. G. Bachmann, F. R. Ahmed, and W. H. Barnes, "The Crystal Structure of Vanadium Pentoxide," Z. Krist. 115 [2] 110-131 (1961).

22. T. I. Barry, "Exploring the Role of Impurities in Non-Metallic Materials by Electron Paramagnetic Resonance," J. Mat. Sci. 4 485-498 (1969).

23. J. B. Goodenough, "Direct Cation-Cation Interactions in Primary Ionic Solids," J. Appl. Phys. Suppl. 31 [5] 359-361 (1960).

24. P. W. Anderson, "Antiferromagnetism.Theory of Superexchange Interaction," Phys. Rev. 79 [4] 705-710 (1950).

25. J. Owen, "Spin Resonance of Ion Pains in Crystal Lattices," J. Appl. Phys. Suppl. 33 [1] 355-357 (1962).

26. L. R. Maxwell and T. R. McGuire, "Antiferromagnetic Resonance," Rev. Mod. Phys. 25 [1] 279-284 (1953).

27. C. M Arya and G. Grossman, Fiz. Tverd. Tela. 2 1283 (1960).

28. D. Adler, "Mechanisms for Metal-Nonmetal Transitions in Transition Metal Oxides and Sulfides," Rev. Mod. Phys. 40 [4] 714-736 (1968).

29. L. L. Hench and D. A. Jenkins, "AC Conductivity of a Glass Semiconductor," Phys. Stat. Sol. 20 [1] 327-330 (1967).

30. A. P. Schmid, "Small Polaron as the Source of Frequency-Dependent Conductivity in Glasses Containing Transition Metal Oxides," J. Appl. Phys. 40 [10] 4128-4136 (1969).

LIST OF FIGURES

LINEWIDTH (GAUSS)
400
350
300
250
200
60
70
80
90
MOLAR PERCENT V_2O_5
UNREDUCED GLASSES
REDUCED GLASSES

Figure 1

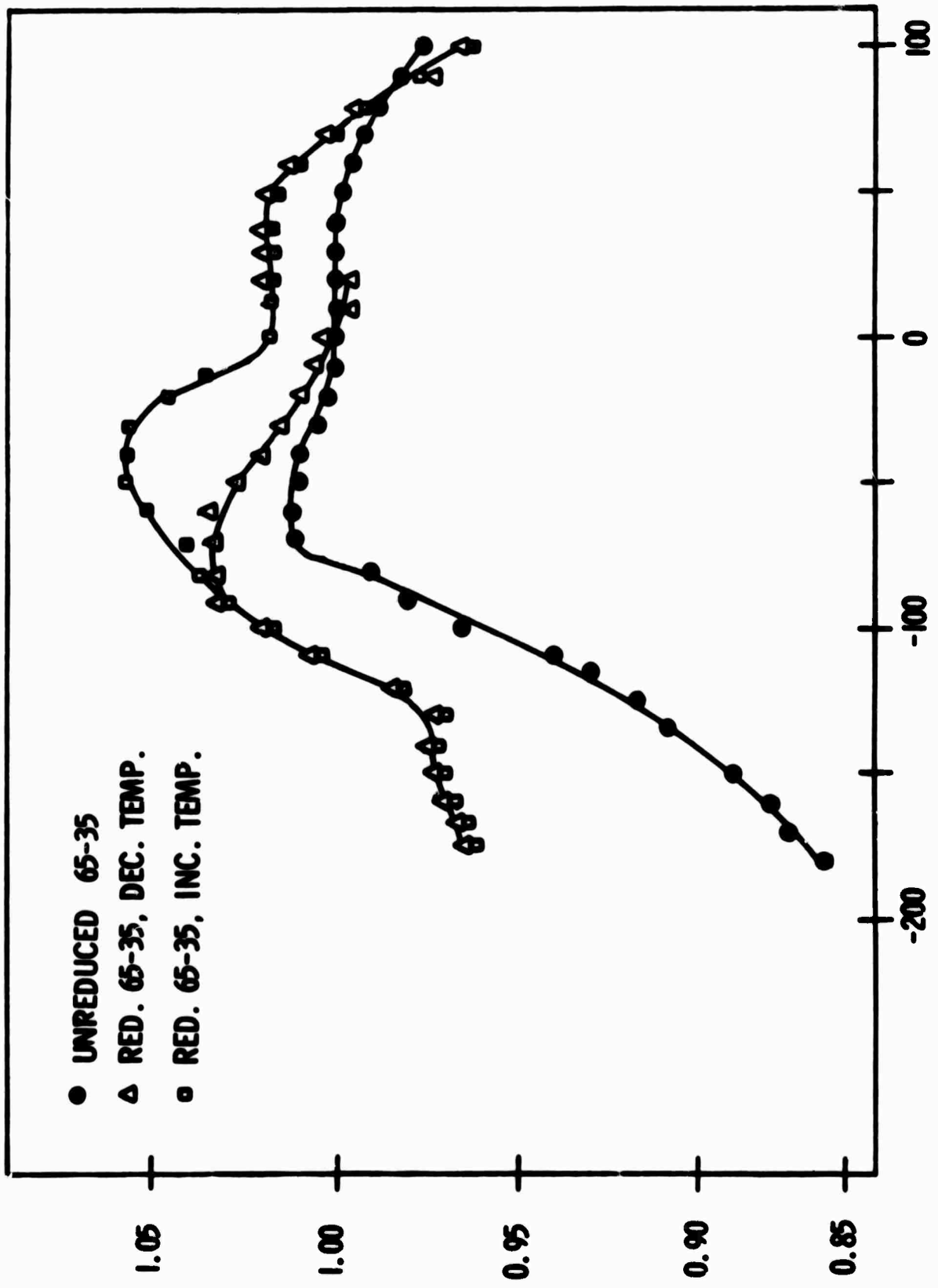
● UNREDUCED 65-35
△ RED. 65-35, DEC. TEMP.
▫ RED. 65-35, INC. TEMP.
1.05
1.00
0.95
0.90
0.85
NORMALIZED INTENSITY
100
0
-100
-200
TEMPERATURE (°C)

Figure 2

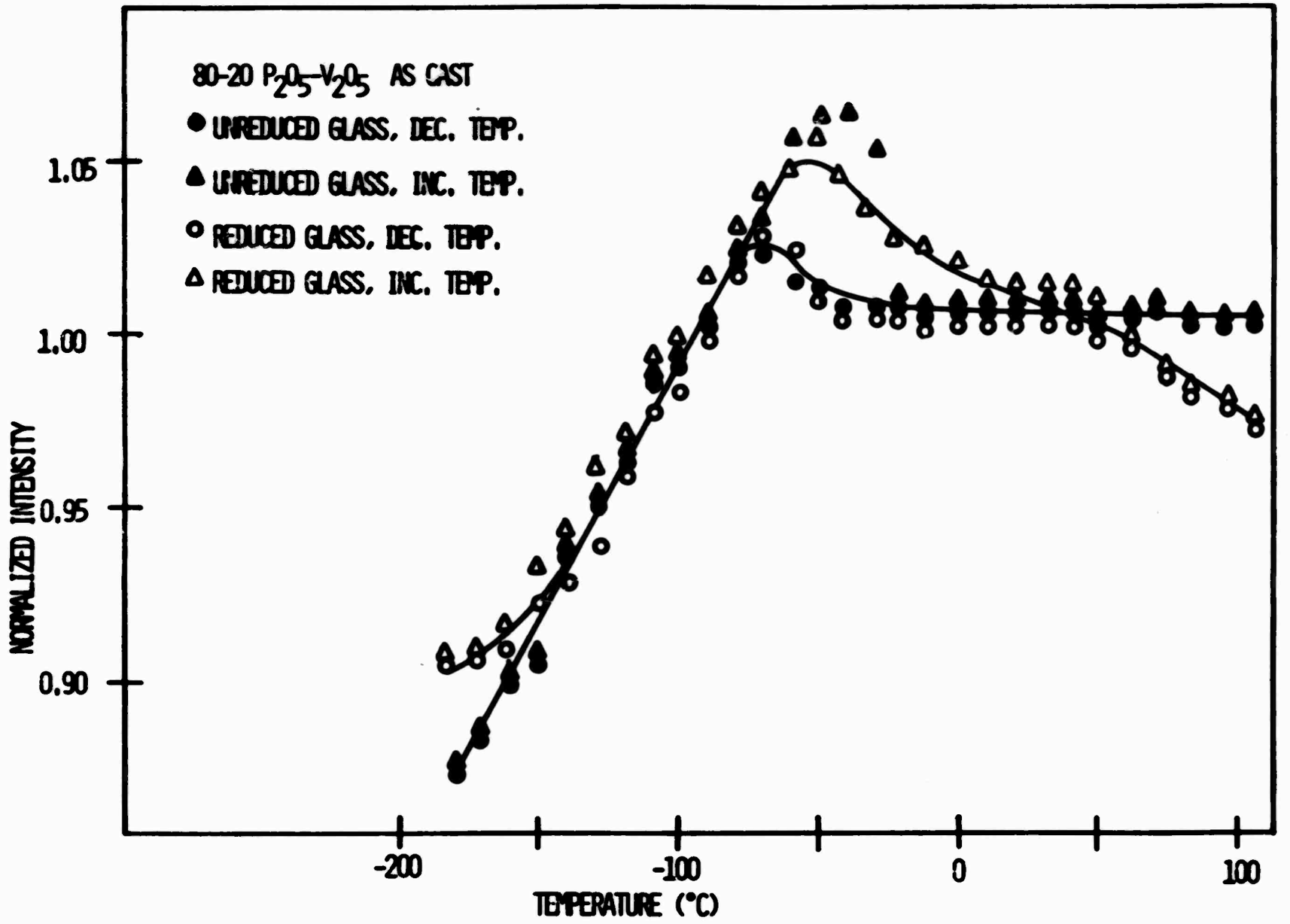
80-20 P_2O_5–V_2O_5 AS CAST
UNREDUCED GLASS, DEC. TEMP.
UNREDUCED GLASS, INC. TEMP.
REDUCED GLASS, DEC. TEMP.
REDUCED GLASS, INC. TEMP.
NORMALIZED INTENSITY
1.05
1.00
0.95
0.90
-200
-100
0
100
TEMPERATURE (°C)

Figure 3

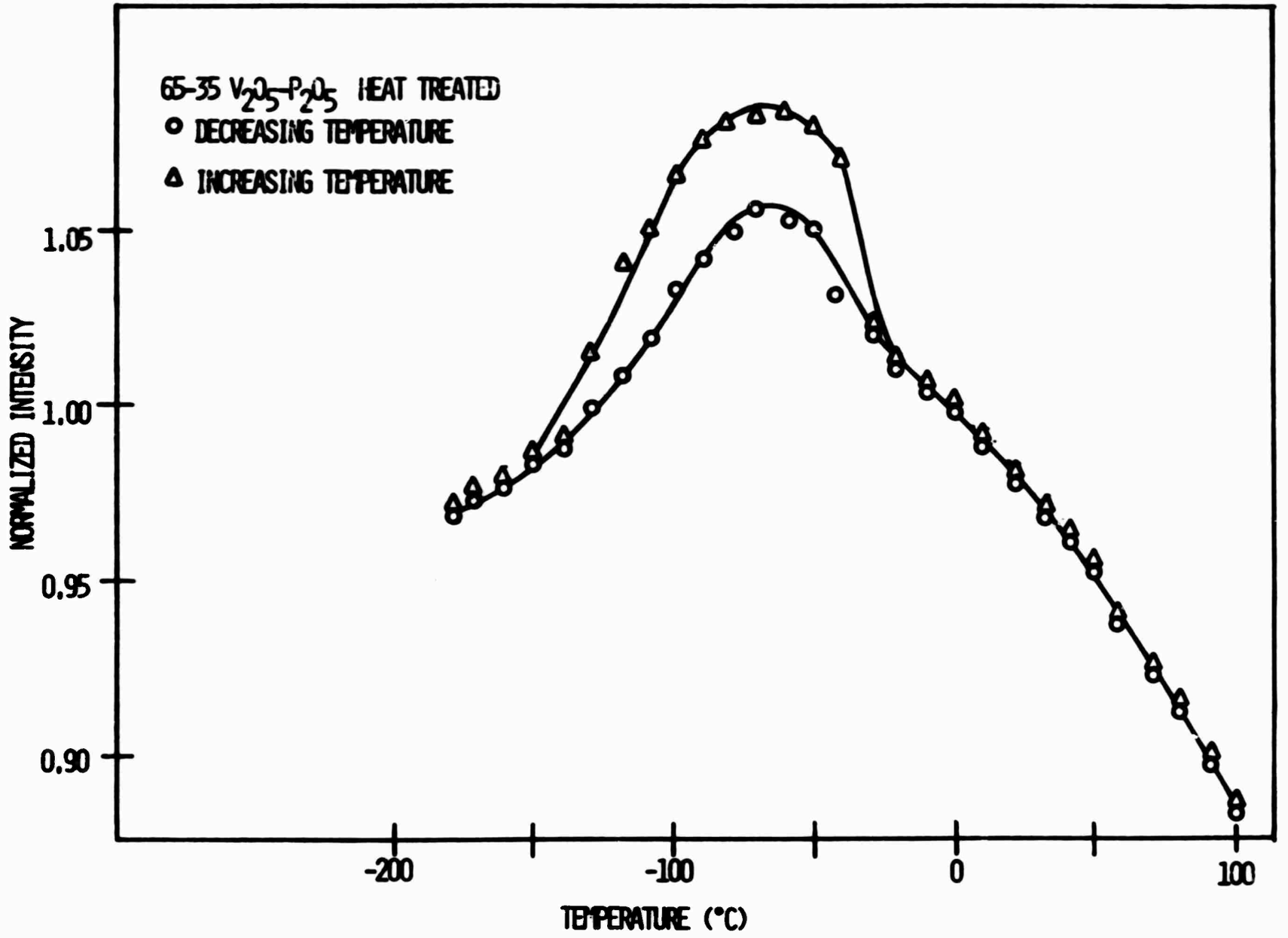
65-35 V_2O_5-P_2O_5 HEAT TREATED
DECREASING TEMPERATURE
INCREASING TEMPERATURE
NORMALIZED INTENSITY
1.05
1.00
0.95
0.90
-200
-100
0
100
TEMPERATURE (°C)

Figure 4

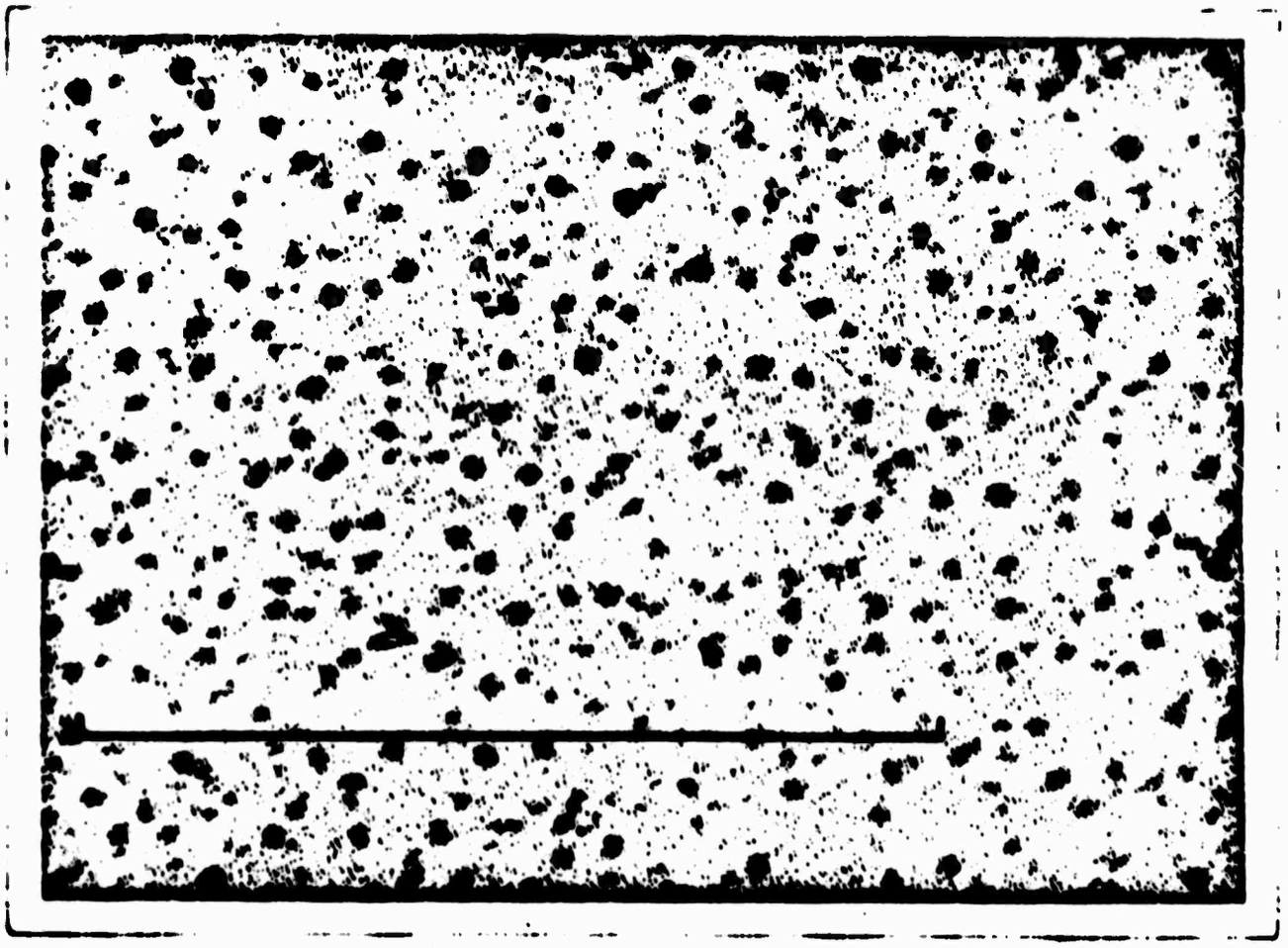

Figure 5

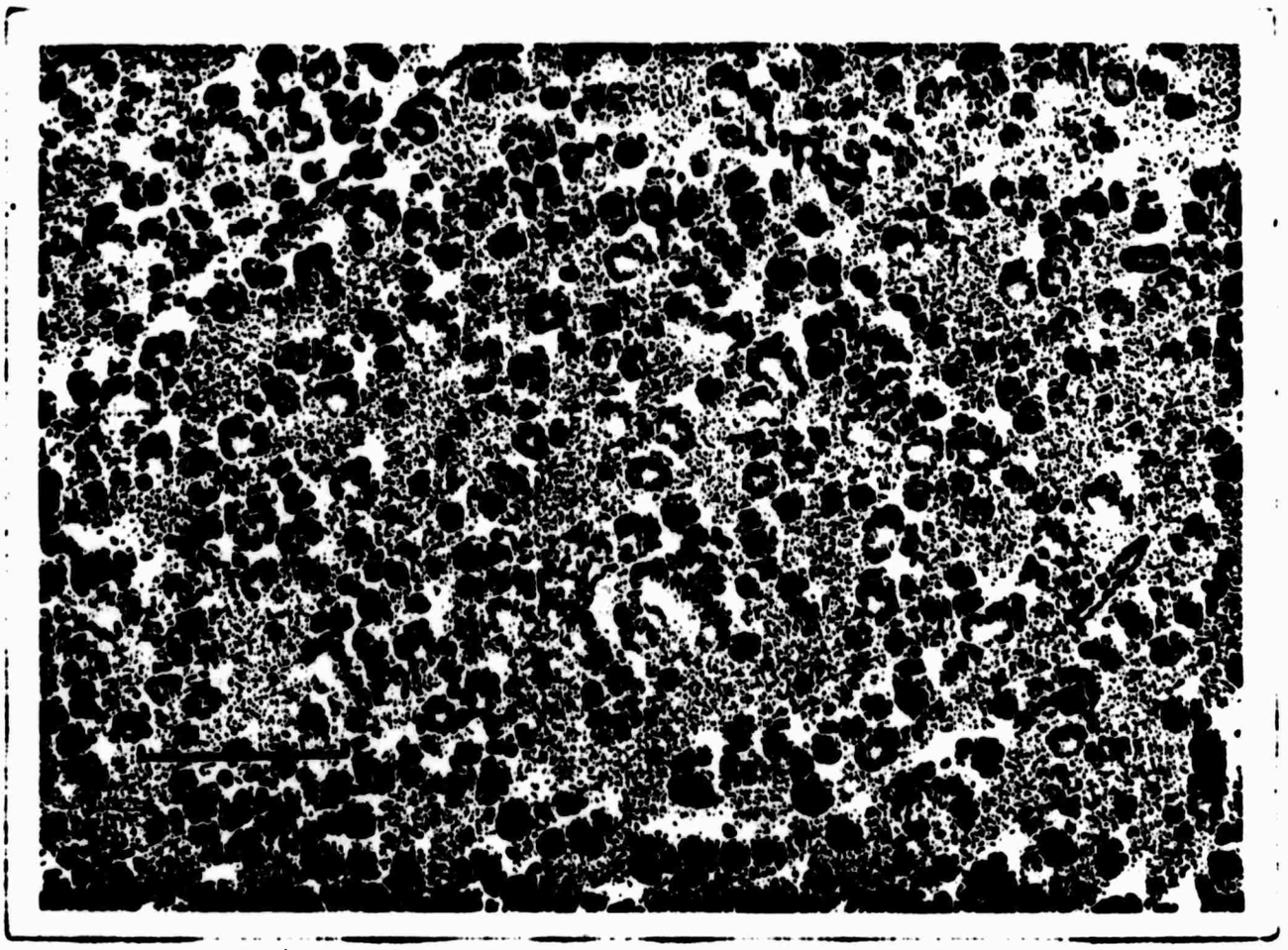

Figure 6

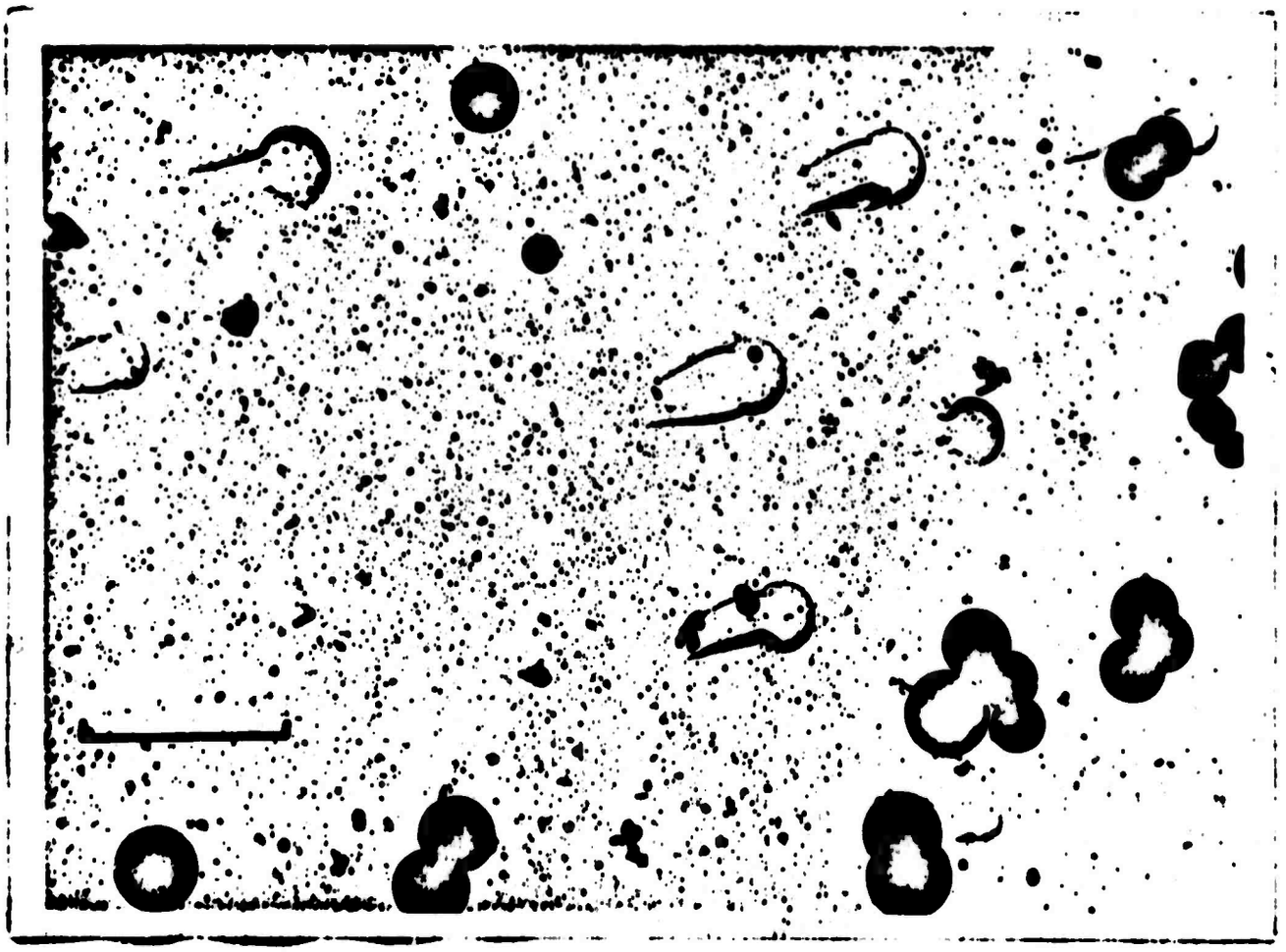

Figure 7

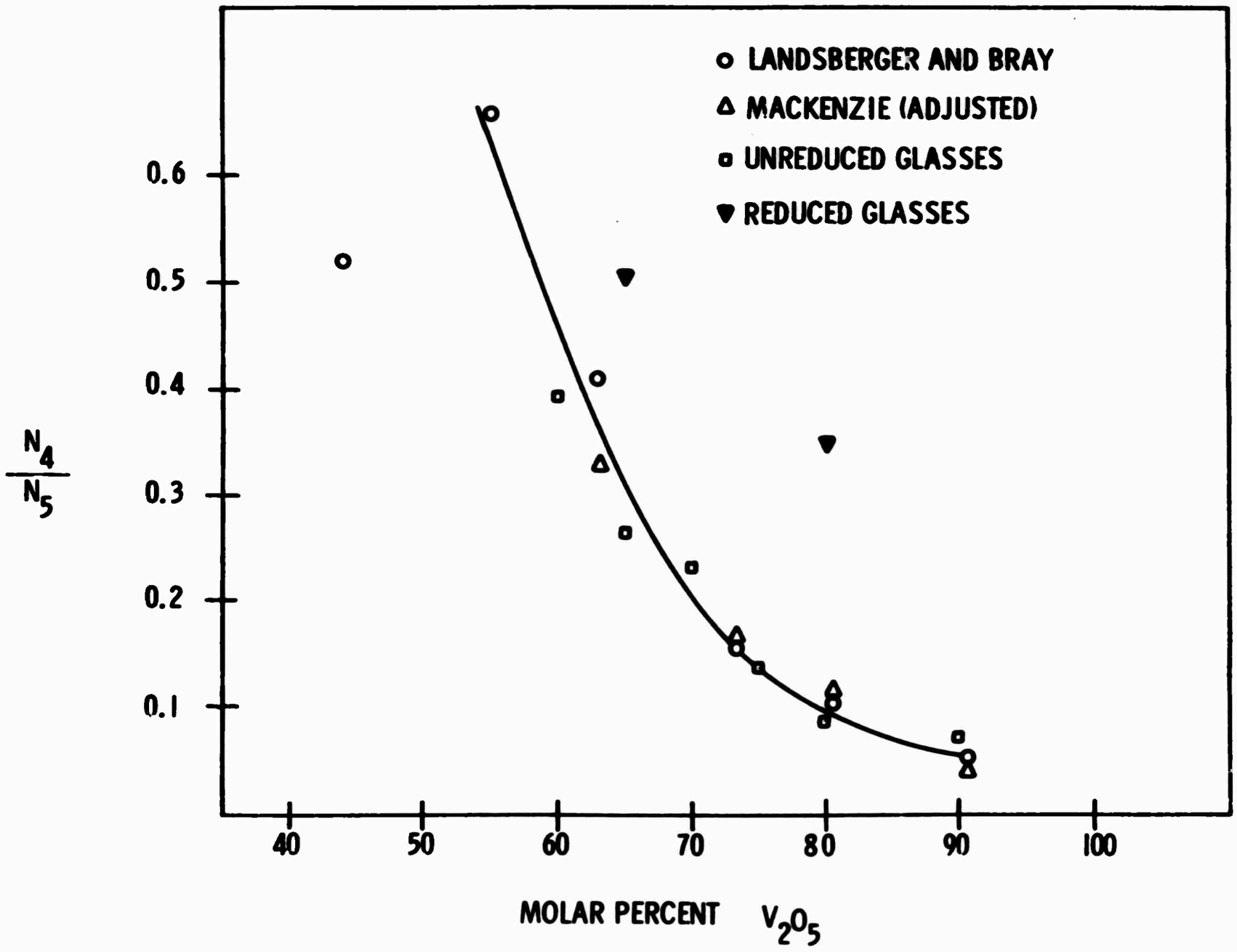
LANDSBERGER AND BRAY
MACKENZIE (ADJUSTED)
UNREDUCED GLASSES
REDUCED GLASSES
0.6
0.5
0.4
0.3
0.2
0.1
$\frac{N_4}{N_5}$
40
50
60
70
80
90
100
MOLAR PERCENT V_2O_5

Figure 8

Figure 9